






# TRIM71 reactivation enhances the mitotic and hair cell-forming potential of cochlear supporting cells

Xiao-Jun Li<sup>1,†</sup> , Charles Morgan<sup>1</sup> , Prathamesh T Nadar-Ponniah<sup>1</sup> , Waldemar Kolanus<sup>2</sup>  & Angelika Doetzlhofer<sup>1,3,\*</sup> 

## Abstract

Cochlear hair cell loss is a leading cause of deafness in humans. Neighboring supporting cells have some capacity to regenerate hair cells. However, their regenerative potential sharply declines as supporting cells undergo maturation (postnatal day 5 in mice). We recently reported that reactivation of the RNA-binding protein LIN28B restores the hair cell-regenerative potential of P5 cochlear supporting cells. Here, we identify the LIN28B target *Trim71* as a novel and equally potent enhancer of supporting cell plasticity. TRIM71 is a critical regulator of stem cell behavior and cell reprogramming; however, its role in cell regeneration is poorly understood. Employing an organoid-based assay, we show that TRIM71 re-expression increases the mitotic and hair cell-forming potential of P5 cochlear supporting cells by facilitating their de-differentiation into progenitor-like cells. Our mechanistic work indicates that TRIM71's RNA-binding activity is essential for such ability, and our transcriptomic analysis identifies gene modules that are linked to TRIM71 and LIN28B-mediated supporting cell reprogramming. Furthermore, our study uncovers that the TRIM71-LIN28B target *Hmga2* is essential for supporting cell self-renewal and hair cell formation.

**Keywords** cochlea; hair cell regeneration; Lin28b; supporting cell reprogramming; Trim71

**Subject Categories** Cell Cycle; RNA Biology; Stem Cells & Regenerative Medicine

**DOI** 10.15252/embr.202256562 | Received 27 November 2022 | Revised 27 June 2023 | Accepted 4 July 2023 | Published online 26 July 2023

**EMBO Reports (2023) 24: e56562**

## Introduction

Mechano-sensory hair cells within the auditory sensory organ (termed cochlea) are essential for our perception of sound. In mammals, auditory hair cells do not regenerate, and their loss or dysfunction is a leading cause of deafness in humans. In non-mammalian vertebrates, such as birds and fish, damaged or lost hair

cells are replenished by their surrounding supporting cells through mitotic and non-mitotic mechanisms (reviewed in Brignull *et al*, 2009). A recent analysis of hair cell regeneration in the zebrafish lateral line revealed that once initiated, hair cell regeneration recapitulates hair cell development (Baek *et al*, 2022). Hair cells and supporting cells in the vertebrate inner ear originate from SOX2 and Jagged1 (JAG1) expressing embryonic progenitor cells termed pro-sensory cells (Kiernan *et al*, 2005; Gu *et al*, 2016). Hair cell fate is determined by the transcription factor ATOH1, which is both necessary and sufficient for hair cell formation (Bermingham *et al*, 1999; Zheng & Gao, 2000). *Atoh1* induction in pro-sensory cells is controlled, among others, by Notch-mediated lateral inhibition and Wnt/ $\beta$ -catenin signaling. Activation of canonical Wnt signaling promotes cell mitosis and activates *Atoh1* expression (Jacques *et al*, 2012; Shi *et al*, 2014), while high levels of Notch signaling inhibit the induction of *Atoh1* expression and force pro-sensory cells to adopt a supporting cell fate (Takebayashi *et al*, 2007). In mice, cochlear hair cells form between embryonic days 14.5 (E14.5) and E18.5. However, many of the developmental gene programs engaged during hair cell formation are still active after birth. For instance, when cultured in the presence of mitogens and a mesenchymal feeder layer, cochlear supporting cells, isolated from early postnatal mice [postnatal day 0 (P0)-P3], readily reenter the cell cycle, proliferate, and form hair cells (White *et al*, 2006; Sinkkonen *et al*, 2011). Hair cell formation by cochlear supporting cells is also induced by inhibition of Notch signaling (Korrapati *et al*, 2013; Mizutari *et al*, 2013) or overactivation of Wnt/ $\beta$ -catenin signaling, which at early postnatal stages also promotes cell cycle reentry of cochlear supporting cells (Chai *et al*, 2012; Shi *et al*, 2012). An even higher potential for mitotic hair cell formation has been demonstrated for Kölliker's cells, which are a transient population of supporting cell-like epithelial cells that reside at the medial border of the cochlear sensory epithelium (Sinkkonen *et al*, 2011; Kubota *et al*, 2021). However, the regenerative potential of cochlear supporting cells and surrounding non-sensory epithelial cells wanes during the first postnatal week, and once mice are hearing, around postnatal day 12 (P12), ectopic activation of *Atoh1* expression or activation of hair cell-fate inducing signals has thus far failed to generate/regenerate functional hair cells (reviewed in Atkinson *et al*, 2015). We recently

1 The Solomon H. Snyder Department of Neuroscience, Johns Hopkins University School of Medicine, Baltimore, MD, USA

2 Molecular Immunology and Cell Biology, Life & Medical Sciences Institute (LIMES), University of Bonn, Bonn, Germany

3 Department of Otolaryngology and Center for Hearing and Balance, Johns Hopkins University School of Medicine, Baltimore, MD, USA

\*Corresponding author. Tel: +1 410 614 9215; Fax: +1 410 614 8033; E-mail: adoetzlhofer@jhmi.edu

†Present address: Frontier Institute of Science and Technology, Xi'an Jiaotong University, Xi'an 710054, China

uncovered a significant role for *let-7* miRNAs and their mutual antagonist LIN28B in the developmental decline in supporting cell plasticity. LIN28B functions as an RNA-binding protein and in the developing cochlea is highly expressed in pro-sensory cells, where it promotes a proliferative, undifferentiated state while differentiating hair cells and supporting cells express members of the *let-7* family of miRNAs, which act to reinforce a post-mitotic terminal differentiated state (Golden et al, 2015). We found that expression of human *LIN28B* in early postnatal cochlear tissue/cells extends the window of hair cell-regenerative capacity, while overexpression of *let-7g* or loss of *Lin28b* (and *Lin28a*) accelerates the developmental decline of regenerative potential (Li & Doetzlhofer, 2020). Our most recent findings indicate that LIN28B enhances the regenerative capacity of cochlear supporting cells and Kölliker's cells by reprogramming them into progenitor-like cells. Among the genes that were induced by LIN28B overexpression was *Trim71* (Li et al, 2022). In the developing cochlear epithelial duct, *Trim71* expression is limited to undifferentiated progenitor cells (Golden et al, 2015). In general, the *Trim71* gene is highly expressed during early embryonic development and functions to promote cell reprogramming and stemness through its dual role as a ubiquitin ligase and RNA-binding protein (Worringer et al, 2014; Torres-Fernandez et al, 2021; Duy et al, 2022). *Lin28b* and *Trim71* are evolutionarily conserved targets of *let-7*-mediated gene silencing (Reinhart et al, 2000; Lin et al, 2007). Recent studies suggest that like LIN28B, TRIM71 interferes with the processing and activity of *let-7* miRNAs (Rybak et al, 2009; Liu et al, 2021; Torres Fernández et al, 2021). Whether the re-expression of *Trim71* enhances the regenerative capacity of cochlear supporting cells has yet to be determined. In this study, we used a cochlear organoid platform as a model to investigate the role of *Trim71* in cochlear-supporting cell plasticity. We show that the functionally related proteins TRIM71 and LIN28B are equally potent enhancers of cochlear supporting cell plasticity. Our mechanistic studies indicate that similar to LIN28B, TRIM71 increases the mitotic and regenerative potential of cochlear supporting cells (and Kölliker's cells) by promoting their de-differentiation into progenitor-like cells. Furthermore, using mutant versions of TRIM71, we find that TRIM71's ability to bind RNA is essential for its positive effect on supporting cell plasticity, while its ubiquitin ligase activity

is dispensable. Our transcriptomic data analysis identifies shared and unique target genes among TRIM71 and LIN28B, and our functional analysis of LIN28B and TRIM71 target gene *Hmga2* reveals that *Hmga2* is essential for the ability of cochlear supporting cells/Kölliker's cells to reenter the cell cycle and form hair cells.

## Results

### Re-expression of TRIM71 increases the mitotic and hair cell-forming potential of cochlear supporting cells

Cochlear supporting cells are post-mitotic cells, and their reentry into the cell cycle is an important aspect of the hair cell regenerative process. To determine whether TRIM71 promotes the reentry of cochlear supporting cells (and Kölliker's cells) into the cell cycle, we expressed human *TRIM71* in cochlear organoid cultures that had been established with cochlear epithelial cells obtained from 5-day-old wild-type mice (postnatal day 5 (P5)). Stage P5 cochlear epithelial cells/supporting cells do still reenter the cell cycle and proliferate but do so at a significantly lower frequency than observed at earlier stages (e.g., P2) when placed in organoid culture (Li & Doetzlhofer, 2020; Li et al, 2022). Briefly, we transduced cochlear epithelial cells with lentiviral particles that expressed full-length TRIM71 (TRIM71) or mutant forms of TRIM71 protein that lacked the RING ( $\Delta$ RING), Coiled-Coil ( $\Delta$ Coiled-Coil), or NHL domain ( $\Delta$ NHL; Fig 1A). The RING domain located within the N-terminal tripartite motif is critical for TRIM71's ubiquitin ligase activity (Rybak et al, 2009), while the coiled-coil domain and C-terminal NHL domain are important hubs for protein interactions and are essential for TRIM71's RNA-binding activity (Loedige et al, 2013). To be able to track transduced cells, the red fluorescent protein mCherry was coexpressed, and to be able to confirm TRIM71 expression, the full-length and mutant TRIM71 proteins contained an N-terminal HA-tag (Fig 1B, and Appendix Fig S1A and B). As a control, cochlear epithelial cells were transduced with lentiviral particles that expressed the HA-tag and mCherry. The transduced cells were then placed at high density into a Matrigel matrix and cultured in the presence of the growth factors EGF and FGF2, GSK3 inhibitor CHIR99021, TGFBR1 inhibitor

**Figure 1. TRIM71 expression increases the mitotic potential of cochlear supporting cells/Kölliker's cells.**

- Schematic of human TRIM71 protein and mutant variants that lack the RING (red,  $\Delta$ RING), Coiled coil (light blue,  $\Delta$ Coiled coil) or NHL domains (dark blue,  $\Delta$ NHL).
- Schematic of lentiviral expression cassette used to express HA-tagged full-length or mutant TRIM71 or HA-tag only (control).
- Experimental scheme. Cochlear epithelial cells from P5 Atoh1-GFP transgenic mice were transduced with mCherry expressing control (Ctrl) lentivirus, or lentivirus that coexpressed mCherry and full-length (TRIM71) or mutant TRIM71 protein ( $\Delta$ RING,  $\Delta$ Coiled Coil,  $\Delta$ NHL) and cultured in expansion media for up to 10 days.
- Bright-field (BF), red (mCherry), and green (Atoh1-nGFP) fluorescent images of organoid cultures after 10 days of expansion. Scale bars = 400  $\mu$ m.
- Colony forming efficiency in (D) ( $n = 4$ , three independent experiments).  $P$ -values were calculated using one-way ANOVA with Tukey's correction. \*\*\*\* $P < 0.0001$ .
- Organoid diameter in (D) ( $n = 4$ , three independent experiments).  $P$ -values were calculated using one-way ANOVA with Tukey's correction. \*\*\*\* $P < 0.0001$ .
- High-power bright-field images of control and TRIM71-expressing organoids after 10 days of expansion. Red arrowheads point to solid, yellow arrowheads to transitional and black arrowheads point to hollow organoids. Scale bar = 400  $\mu$ m.
- Organoid types in (G) ( $n = 5$ , two independent experiments).  $P$ -values were calculated using two-tailed, unpaired  $t$  test. \* $P \leq 0.05$ , \*\* $P < 0.01$ .  $P > 0.5$  deemed not significant (n.s.).
- High-power single-plane confocal images of EdU labeled control and TRIM71-expressing organoids. An EdU pulse was given on day 8 and EdU incorporation (green) was analyzed 1.5 h later. JAG1 immunostaining (magenta) marks supporting cells/prosensory cells, mCherry (red) marks transduced cells, and Hoechst labels cell nuclei (blue). Scale bar = 25  $\mu$ m.
- Percentage of EdU<sup>+</sup> mCherry<sup>+</sup> cells per organoids in (I); ( $n = 5$ , two independent experiments).  $P$ -values were calculated using two-tailed, unpaired  $t$  test. \*\* $P < 0.01$ .

Data information: Plotted are individual data points, representing the average value per animal and treatment, and mean  $\pm$  standard deviation (SD) of biological replicates.

Source data are available online for this figure.

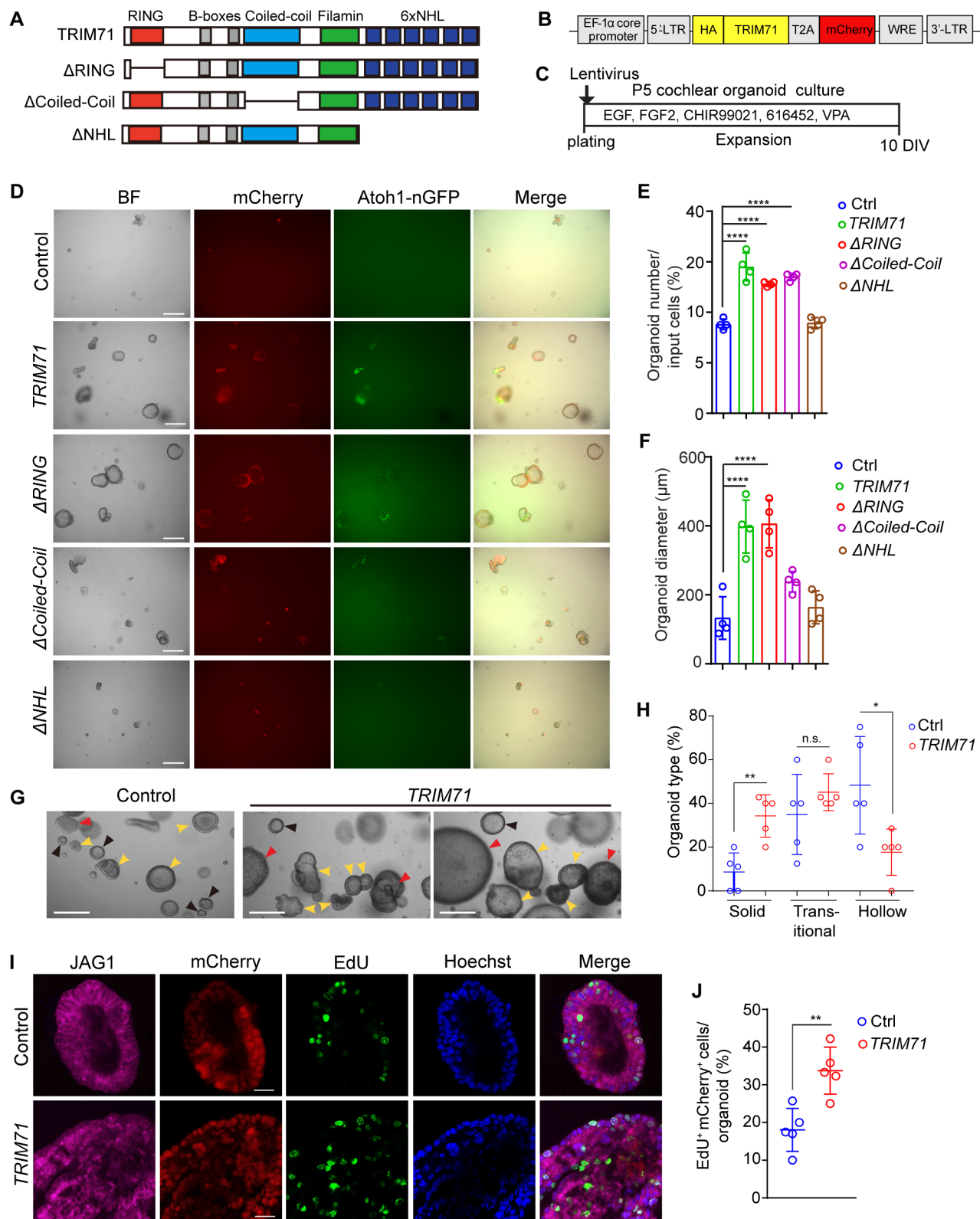


Figure 1.

616452, and HDAC inhibitor valproic acid (VPA) for 10 days (Fig 1C). We found that TRIM71 expression increased organoid formation efficiency (colony forming efficiency) by 1.5-fold compared

to control (Fig 1D and E) and increased the average organoid diameter by twofold compared to control (Fig 1D and F). Expression of TRIM71 protein that lacked the RING domain ( $\Delta$ RING) had a similar

positive effect as expression of full-length TRIM71 protein, indicating that TRIM71 does not require its E3 ubiquitin ligase activity to promote organoid formation and growth (Fig 1D–F). By contrast, expression of TRIM71 protein that lacked the NHL domain ( $\Delta$ NHL) failed to increase organoid formation or organoid size compared to the control (Fig 1D–F), indicating that the RNA-binding domain is required for TRIM71's positive effect on organoid formation and growth. An intermediate phenotype was observed in cultures that expressed Coiled-Coil domain deficient TRIM71 protein ( $\Delta$ Coiled-Coil), with no defects in organoid formation but a mild reduction in organoid growth (Fig 1D–F).

Closer inspection of TRIM71-expressing organoids and control organoids revealed striking differences in their morphologies (Fig 1G). Cochlear organoids can be classified as solid, hollow, or transitional, with solid organoids having the highest capacity for hair cell production and hollow organoids the lowest (Kubota et al, 2021). Applying similar criteria for classification, we found that TRIM71-expressing organoid cultures contained a significantly higher percentage of solid organoids and a significantly lower percentage of hollow organoids than control cultures, whereas the number of transitional organoids remained unchanged (Fig 1H). To determine whether the TRIM71-induced changes in organoid size and morphology were a consequence of increased cell proliferation, we pulsed control and TRIM71-expressing cultures with EdU and analyzed the percentage of transduced cells per organoid that incorporated EdU. To verify supporting cells/Kölliker's cell identity, cultures were also stained for Notch ligand Jagged1 (JAG1), which is highly expressed in supporting cells/Kölliker's cells and their precursors. We found that more than 95% of cells in control and TRIM71-expressing cultures expressed JAG1 (Fig 1I), confirming that most organoids are composed of supporting cells/Kölliker's cells or their precursors. As anticipated, we found that the percentage of EdU<sup>+</sup> mCherry<sup>+</sup> cells in TRIM71-expressing organoids was twofold increased (Fig 1I and J), indicating TRIM71 as a positive regulator of supporting cell/Kölliker's cell proliferation.

We next examined whether the expression of TRIM71 enhances the hair cell-forming capacity of stage P5 cochlear supporting cells/Kölliker's cells. At stage P5, cochlear epithelial cells (supporting cells and Kölliker's cells) still produce some hair cells in organoid culture, but the rate of hair cell production is greatly reduced compared to earlier stages (e.g., P2; Li & Doetzlhofer, 2020; Li et al,

2022). To be able to monitor the dynamics of hair cell formation in our cultures, we used cochlear epithelial cells from *Atoh1-nGFP* transgenic mice, which express nuclear GFP in nascent hair cells. To stimulate hair cell formation, organoids were cultured in a “differentiation media” that contained GSK-3 $\beta$  inhibitor CHIR99021 (activates Wnt signaling) and  $\gamma$ -secretase inhibitor LY411575 (inhibits Notch signaling; Fig 2A). We found that after 2 days of differentiation, about 40% of TRIM71-expressing organoids contained clusters of nascent hair cells (Atoh1-GFP<sup>+</sup> cells), while only about 5% of control organoids contained nascent hair cells (Fig 2B and C). Expression of TRIM71 protein that lacked the RING domain ( $\Delta$ RING) was equally effective in promoting hair cell formation as full-length TRIM71 protein. By contrast, TRIM71 proteins that lacked either the Coiled-Coil domain ( $\Delta$ Coiled-Coil) or the NHL ( $\Delta$ NHL) domain were ineffective in inducing hair cell formation (Fig 2B and C). The positive effect of TRIM71 on hair cell formation was confirmed by analyzing *Atoh1* mRNA expression using RT-qPCR. We found that expression of full-length or RING domain deficient TRIM71 protein resulted in a 4–8-fold increase in *Atoh1* mRNA abundance compared to control, while *Atoh1* mRNA levels remained unchanged by the expression of NHL or Coiled-Coil domain deficient TRIM71 protein compared to control (Fig 2D). The hair cell identity of Atoh1-nGFP<sup>+</sup> cells in TRIM71-expressing organoids was confirmed using immunostaining against the hair cell-specific protein myosin VIIa (MYO7A; Fig 2E and F). Furthermore, we found that TRIM71 expression increased *Myo7a* mRNA expression by more than threefold compared to control, while expression of TRIM71 protein that lacked the NHL domain failed to increase *Myo7a* expression (Fig 2G). In sum, our organoid culture experiments suggest that TRIM71's ability to bind RNA is essential for boosting the mitotic and hair cell-forming capacity of cochlear supporting cells and Kölliker's cells, whereas TRIM71's ubiquitin ligase activity is dispensable.

To be able to test whether re-expression of TRIM71 boosts hair cell production in intact cochlear tissue, we engineered adeno-associated viral (AAV) particles that express HA-tag only (AAV-Ctrl) or express HA-tagged human TRIM71 (AAV-TRIM71) using the Anc80L65 capsid protein. In contrast to lentiviruses, AAVs, in particular AAVs of the Anc80L65 serotype, are highly effective in transducing hair cells and supporting cells in intact cochlear tissue (Landegger et al, 2017). For our experiment, we isolated cochlear

### Figure 2. TRIM71 expression increases the hair cell-forming potential of cochlear supporting cells/Kölliker's cells.

- A Experimental scheme. Cochlear epithelial cells from P5 *Atoh1-nGFP* transgenic mice were transduced with mCherry expressing control (Ctrl) lentivirus, or lentivirus that co-expressed mCherry and full-length (TRIM71) or mutant TRIM71 protein ( $\Delta$ RING,  $\Delta$ Coiled Coil,  $\Delta$ NHL) and cultured in differentiation media for 2 days following expansion.
- B Bright field (BF), red (mCherry) and green (Atoh1-nGFP) fluorescent images of organoid cultures after 2 days of differentiation. Scale bar = 400  $\mu$ m.
- C Percentage of Atoh1-nGFP<sup>+</sup>mCherry<sup>+</sup> organoids in (B) ( $n = 5$ , three independent experiments).  $P$ -values were calculated using one-way ANOVA with Tukey's correction. \*\*\*\* $P < 0.0001$ .
- D RT-qPCR of *Atoh1* mRNA in organoids ( $n = 3$ , two independent experiments).  $P$ -values were calculated using one-way ANOVA with Tukey's correction. \*\*\*\* $P < 0.0001$ .
- E High-power single-plane confocal images of MYO7A immuno-stained (magenta) organoids. Atoh1-GFP (green) and MYO7A (magenta) mark nascent hair cells. MCherry (red) marks transduced cells. Scale bar = 20  $\mu$ m.
- F Quantification of MYO7A<sup>+</sup> mCherry<sup>+</sup> cells per organoid in (E) ( $n = 3$ , two independent experiments).  $P$ -values were calculated using one-way ANOVA with Tukey's correction.  $P > 0.5$  is deemed not significant (n.s.).
- G RT-PCR of *Myo7a* mRNA expression in organoids ( $n = 3$ , two independent experiments).  $P$ -values were calculated using one-way ANOVA with Tukey's correction. \* $P \leq 0.05$ .

Data information: Plotted are individual data points, representing the average value per animal and treatment, and mean  $\pm$  SD of biological replicates. Source data are available online for this figure.



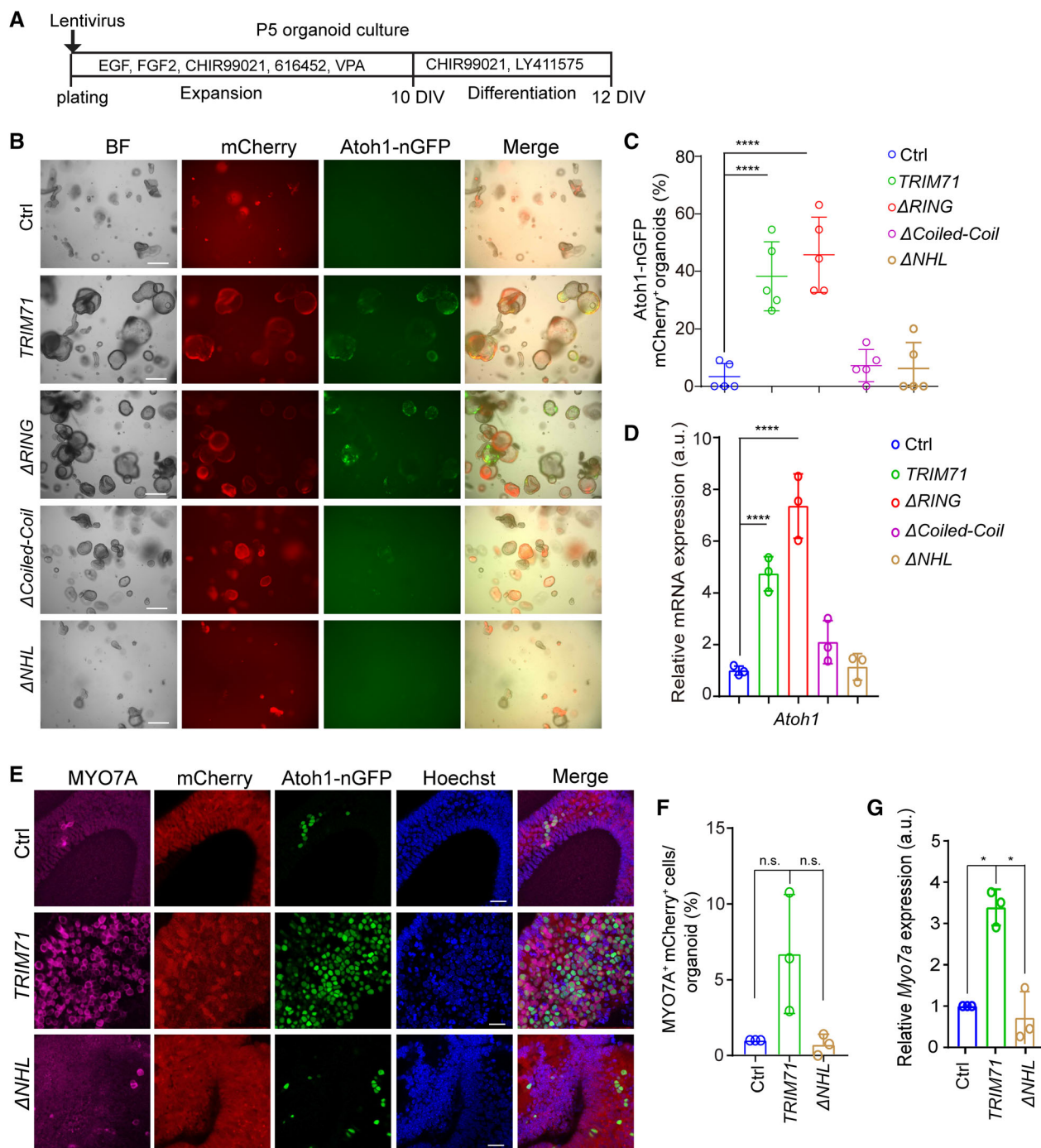


Figure 2.

tissue from stage P2 wild-type mice and cultured the cochlear explants in the presence of control or *TRIM71*-expressing AAV for 48 h. After 48 h of culture, which corresponds to stage P4/P5, we treated control and *TRIM71*-expressing cochlear explants with  $\gamma$ -secretase inhibitor LY411575 (inhibits Notch signaling), and after a total of 6 days in culture, explants were stained for MYO7A and SOX2, which mark newly formed hair cells (Fig EV1A and B). Our analysis revealed that re-expression of *TRIM71* in early postnatal cochlear explants increases the rate of new hair cell formation

(MYO7A<sup>+</sup> SOX2<sup>+</sup> cells) in response to Notch inhibition by more than twofold compared to control (Fig EV1B and C). Viral *TRIM71* expression was confirmed by analyzing *TRIM71* mRNA and protein expression using RT-qPCR and western blot analysis (Fig EV1D and E).

*Trim71* is abundantly expressed in undifferentiated cochlear epithelial cells, but its expression rapidly declines at the onset of differentiation and is near undetectable after birth (Golden *et al.*, 2015; Evsen *et al.*, 2020; Kolla *et al.*, 2020). To determine whether endogenous *Trim71* is essential for supporting cells to reenter the cell cycle

and form new hair cells, we deleted *Trim71* in P2 cochlear organoid cultures. We selected stage P2 for our *Trim71* loss-of-function experiments as at this stage wild-type cochlear epithelial cells, as well as FACS-purified cochlear supporting cells/Kölliker's cells, readily form large hair cell-containing organoids (McLean et al, 2017; Li & Doetzlhofer, 2020; Kubota et al, 2021; Li et al, 2022). To knockout (KO) *Trim71*, we used *Trim71* floxed (*Trim71<sup>fl/fl</sup>*) mice in which upon Cre-mediated recombination exon 4 (codes for the NHL-domain) is removed (Mitschka et al, 2015; Fig 3A). The *Trim71* floxed mice also carried *R26<sup>rtTA\*</sup>M2* and *TetO-Cre* transgenes, which enable doxycycline-mediated Cre induction (Fig 3A). Doxycycline-mediated Cre induction in *Trim71<sup>fl/fl</sup> R26<sup>rtTA\*</sup>M2 TetO-Cre* embryos at around E5.5 causes severe neural tube closure defects, and embryos die at E13.5/E14.5 (Duy et al, 2022). Similar defects have been reported for non-conditional *Trim71* mutant mouse lines, which contain a gene trap vector in intron 1 (Maller Schulman et al, 2008) or intron 2 (Cuevas et al, 2015), suggesting that loss of exon 4 is equivalent to a complete loss of gene function.

As control, we used littermates that lacked the *TetO-Cre* transgene. To induce *Trim71* deletion we expanded *TetO-Cre; R26<sup>rtTA\*</sup>M2; Trim71<sup>fl/fl</sup>* (subsequently referred to as *Trim71* KO), and *Trim71<sup>fl/fl</sup>; R26<sup>rtTA\*</sup>M2* (control, wild type) cochlear epithelial cells in the presence of doxycycline (dox; Fig 3B). After 6 days of expansion, we analyzed organoid formation efficiency and organoid size in control and *Trim71* KO cultures. Our analysis revealed no defects in organoid formation or organoid growth in the absence of *Trim71* (Fig 3C–E). Furthermore, 1.5-h EdU pulse at 7 days of expansion revealed no significant changes in the rate of cell proliferation in *Trim71* KO organoids compared to control (Fig 3F and G). By contrast, organoid cultures established with cochlear epithelial cells isolated from E13.5 *Trim71* KO embryos that were cultured in identical conditions (Fig EV2A) formed significantly fewer and smaller organoids (Fig EV2B–D) and incorporated EdU at a significantly lower rate than control cultures established from wild-type littermates (Fig EV2E and F). These results indicate that *Trim71* function is essential for cell cycle reentry and proliferation of undifferentiated

cochlear epithelial cells (pro-sensory cells), but its function is not required for the cell cycle reentry and proliferation of cochlear supporting cells (and Kölliker's cells).

### Loss of *Trim71* attenuates the hair cell-forming capacity of cochlear supporting cells/Kölliker's cells

We next analyzed whether loss of *Trim71* impacts the hair cell-forming capacity of cochlear progenitor cells and supporting cells/Kölliker's cells. Our analysis revealed that while organoid cultures established with E13.5 wild-type cochlear epithelial cells readily produced Atoh1-nGFP<sup>+</sup> hair cells, organoid cultures established with E13.5 *Trim71* deficient cochlear epithelial cells failed to produce Atoh1-nGFP<sup>+</sup> hair cells (Fig EV2G and H). Much milder defects in hair cell formation were observed in *Trim71* KO organoid cultures established with P2 cochlear epithelial cells.

We found that after 2 days of differentiation, P2 *Trim71* KO organoids expressed hair cell-fate-inducing genes (*Atoh1*, *Pou4f3*) on average at a twofold lower level than control organoids (Fig 3H and I). After 6 days of differentiation, the majority of Atoh1-nGFP<sup>+</sup> cells in control organoids coexpressed hair cell-specific protein MYO7A. By contrast, Atoh1-nGFP<sup>+</sup> cells in *Trim71* KO organoids lacked MYO7A expression (Fig 3J). We observed qualitative similar defects in hair cell formation when we used Cre expressing lentiviral particles to delete *Trim71* in stage P2 cochlear organoid culture (Appendix Fig S2A and B). RT-qPCR revealed that hair cell-specific genes (*Myo7a*, *Pou4f3*) were expressed at a significantly lower level in *Trim71* KO organoids than control organoids (Appendix Fig S2C). To determine whether the defects in hair cell formation were due to defects in supporting cell reprogramming or due to defects in hair cell-fate induction, we analyzed the expression of progenitor cell, supporting cell, and hair cell-specific genes in P2 control and *Trim71* KO cochlear organoids during expansion using RT-qPCR. Our analysis revealed that *Trim71* KO organoids expressed progenitor-specific genes (*Fat3*, *Ccnd2*, *Fst*) at a lower level and supporting cell-specific genes (*Ano1*, *Cybrd1*, *S100a1*) at a higher

**Figure 3. Loss of *Trim71* attenuates the hair cell-forming capacity of cochlear supporting cells/Kölliker's cells.**

- A Schematic of conditional knockout strategy for murine *Trim71*.
- B Experimental scheme for (C–G). Cochlear epithelial cells from P2 *TetO-Cre; R26<sup>rtTA\*</sup>M2; Trim71<sup>fl/fl</sup>* mice (*Trim71* KO) and littermates that lacked *TetO-Cre* transgene (wild type, WT) were cultured in expansion media in the presence of doxycycline (dox).
- C Bright-field (BF) images of WT and *Trim71* KO organoid culture after 6 days of expansion. Scale bars = 400  $\mu$ m.
- D Colony forming efficiency in (C) ( $n = 4$  in WT,  $n = 5$  in *Trim71* KO, two independent experiments). A two-tailed, unpaired *t* test was used to calculate *P* values. n.s., not significant.
- E Organoid diameter in (C) ( $n = 4$  in WT,  $n = 5$  in *Trim71* KO, two independent experiments). A two-tailed, unpaired *t*-test was used to calculate *P* values. n.s., not significant.
- F High-power single-plane confocal images of EdU (red) and Hoechst (blue) labeled WT and *Trim71* KO organoids. A single EdU pulse was given on day 7 and EdU incorporation was analyzed 1.5 h later. Scale bars = 25  $\mu$ m.
- G Percentage of EdU<sup>+</sup> cells in (F) ( $n = 15$  in WT,  $n = 11$  in *Trim71* KO, three independent experiments). A two-tailed, unpaired *t* test was used to calculate *P* values, n.s. not significant.
- H Experimental scheme for (I, J). Organoids were established as in (B), and following expansion, cultured in differentiation media for up to 6 days.
- I RT-qPCR of *Trim71* and progenitor (*Hmag2* and *Fat3*) and hair cell-specific (*Atoh1*, *Gfi1*, and *Pou4f3*) mRNAs in control and *Trim71* KO organoids at day 10 ( $n = 4$  in WT,  $n = 5$  in *Trim71* KO, two independent experiments). A two-tailed, unpaired *t* test was used to calculate *P* values. \*\**P* < 0.01, \*\*\*\**P* < 0.0001.
- J RT-qPCR of *Trim71* and hair cell-specific (*Atoh1*, *Gfi1*, and *Pou4f3*) mRNAs in WT and *Trim71* KO organoids after 2 days of differentiation ( $n = 3$ , two independent experiments). A two-tailed, unpaired *t*-test was used to calculate *P* values. \**P* < 0.05.
- K High-power single plane confocal images of MYO7A and SOX2 immuno-stained WT and *Trim71* KO organoids after 6 days of differentiation. Nascent hair cells coexpress Atoh1-nGFP (green), MYO7A (red), and SOX2 (magenta). Scale bars = 25  $\mu$ m.

Data information: Plotted are individual data points, representing the average value per animal and treatment, and mean  $\pm$  SD of biological replicates. Source data are available online for this figure.

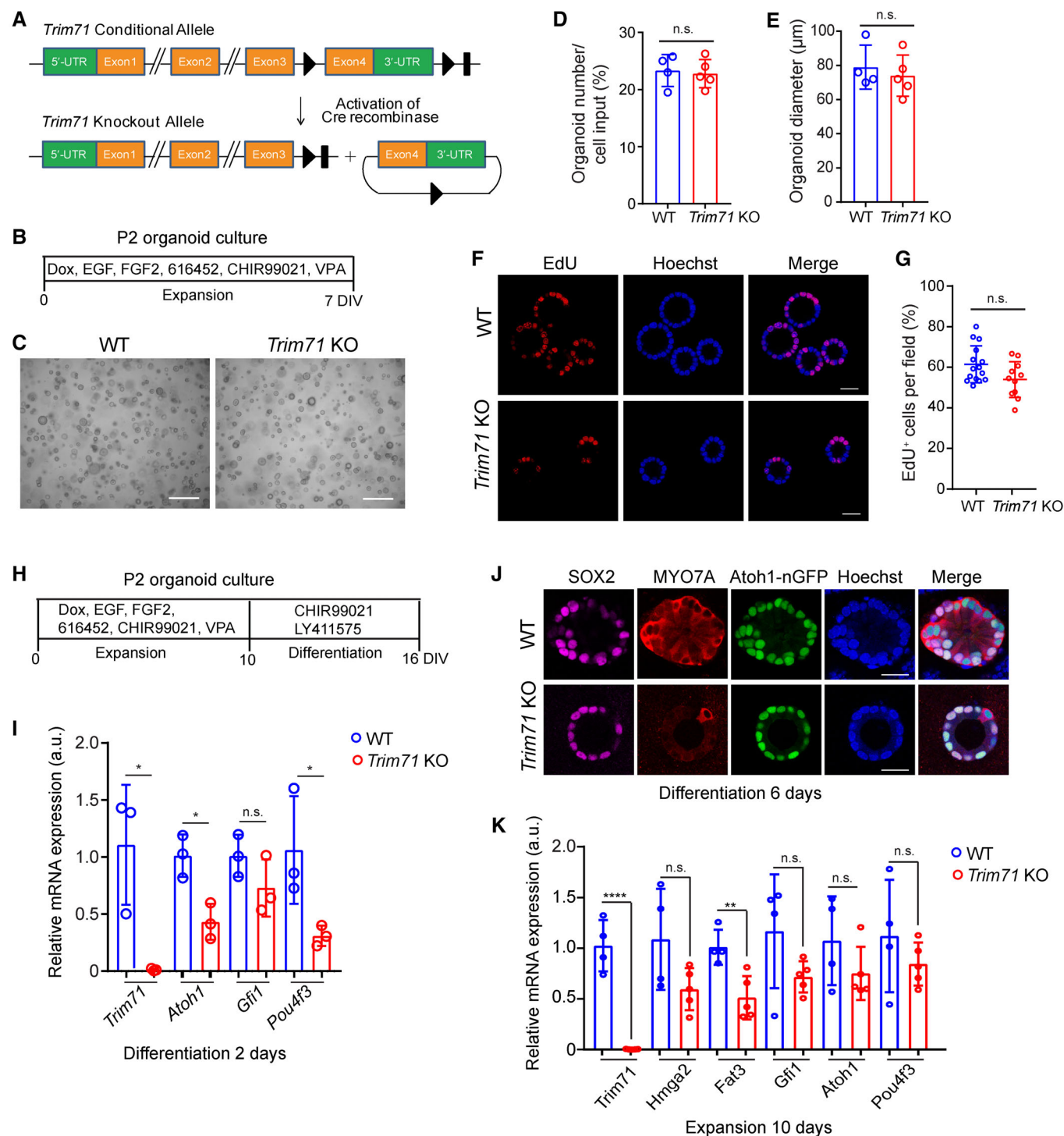


Figure 3.

level than control organoids (Fig 3K and Appendix Fig S2D), while the initial induction of hair cell-fate inducing genes (*Atoh1*, *Pou4f3*, *Gfi1*) was unaffected (Fig 3K). In sum, our results indicate that prior differentiation *Trim71* is essential for cochlear pro-sensory cells to self-renew and form hair cells and that at later, perinatal stages *Trim71* is dispensable for self-renewal but plays a positive role in the reprogramming of supporting cells into progenitor-like cells and the subsequent formation of hair cells.

### TRIM71 increases the expression of genes linked to self-renewal and de-differentiation in cochlear supporting cells/Kölliker's cells

To uncover the underlying mechanism through which TRIM71 enhances the mitotic and hair cell regenerative capacity of supporting cells/Kölliker's cells, we analyzed the transcriptome of P5 control and *TRIM71*-expressing cochlear organoids at the end of the expansion phase using RNA-sequencing (RNA-seq). Briefly,

we transduced cochlear epithelial cells isolated from P5 wild-type mice with control or *TRIM71*-expressing lentiviral particles and expanded these cells as organoids for 10 days. To quantify transcript abundance, we pseudo-align reads to the reference mouse transcriptome (Ensembl Mus musculus v96), using Kallisto (v0.46.1; Bray et al, 2016). We used the companion tool sleuth to determine differentially expressed genes (DEGs) by comparing the control to the *TRIM71*-expressing condition (Pimentel et al, 2017). Our analysis identified 2,883 DEGs ( $q$ -value < 0.01; Dataset EV1), with 1,500 upregulated and 1,383 downregulated genes in response to *TRIM71* expression. Among the *TRIM71*-upregulated genes were genes that function in pro-sensory cell specification and maintenance (*Hey1*, *Hey2*, *Bmp4*, *Id2*, *Sox11*, *Fgf9*) as well as genes that are induced during hair cell formation (*Atoh1*, *Prox1*, *Rbm24*; Fig 4A, red dots). By contrast, the list of *TRIM71*-downregulated genes included genes critical for cell adhesion (*Chd1*, *Col11a1*, *Col11a2*) and glial cell differentiation (*Zbtb20*, *Nfib*, *Nfix*, *Sox21*), including *Nfix*, which has been recently shown to be directly bound by *TRIM71* (Foster et al, 2020; Fig 4A, blue dots). To identify the biological processes and pathways that may be altered by *TRIM71* expression, we performed a gene ontology enrichment analysis using Metascape, a web-based portal (<https://metascape.org>; Zhou et al, 2019). Consistent with *TRIM71*'s role as a stemness and pluripotency factor, we found that the list of *TRIM71*-upregulated genes was significantly enriched for genes that promote cell cycle reentry and mitosis, regulate the response to DNA damage, and inhibit cell differentiation (Fig 4B and Dataset EV2), while the list of *TRIM71*-downregulated genes was significantly enriched for genes that function in cell adhesion, external structure organization as well as actin filament-based processes and organization (Fig 4C and Dataset EV2).

#### TRIM71 regulates gene expression in a *let-7* independent manner

LIN28B and *TRIM71* proteins are known to enhance each other's expression and to share many of the same downstream targets (Robinton et al, 2019; Foster et al, 2020). To identify common as well as unique targets of *TRIM71* and LIN28B in supporting cells/Kölliker's cells, we compared the RNA-seq data with our recently published RNA-seq data that profiled the effects of LIN28B on supporting cell/Kölliker's cell gene expression in P5 cochlear organoid culture in the presence of follistatin (FST), which we used in lieu of a TGFBR inhibitor (Li et al, 2022). The data comparison revealed that close to one-third of LIN28B + FST-upregulated or

downregulated genes were in a similar fashion up or downregulated by *TRIM71* expression (Dataset EV3). The shared list of upregulated genes included well-known *let-7* targets such as *Hmga2*, *Arid3a*, *Igf2bp1*, *Ccnd2*, and *Trim71* itself (Dataset EV3 and Fig 4D), suggesting that in cochlear organoid culture, *TRIM71* may inhibit the expression or activity of mature *let-7* miRNAs or both.

Among the cohort of genes that were upregulated by *TRIM71* but not by *LIN28B* expression were BMP-responsive genes (*Bmp4*, *Id2*, *Msx1*, *Msx2*; Fig 4D). During cochlear development, BMP signaling is essential for pro-sensory cell fate specification (Ohyama et al, 2010), suggesting that strengthening BMP signaling could be a key mechanism through which *TRIM71* enhances supporting cell plasticity. Correlating with the ability of *TRIM71* variants to enhance cell proliferation and hair cell formation, we found that expression of full-length or RING-domain deficient *TRIM71* protein increased the expression of BMP-responsive genes (*Bmp4*, *Id2*, and *Id3*), whereas no changes in the expression of BMP-responsive genes were observed in response to expression of NHL deficient or Coil-Coil deficient *TRIM71* proteins (Figs 4E and EV3A). We next analyzed the level of phosphorylated (p)-SMAD1/5/9 proteins, an indicator of BMP signal strength, in control organoids and organoids that expressed full-length or NHL-deficient *TRIM71* protein. As positive controls, we also analyzed protein levels of *TRIM71* target genes *Hmga2* and *Lin28b*. As anticipated, our analysis revealed that *TRIM71* expression increased BMP signaling in cochlear organoids and showed that *TRIM71*'s positive effect on BMP signaling requires a functional NHL domain (Fig 4F).

Recent studies found that *TRIM71* represses the expression of mature *let-7* miRNAs by binding LIN28A or LIN28B proteins and enhancing their inhibition of *let-7* biogenesis (Torres Fernández et al, 2021). Our pull-down experiments using HEK293T cells revealed that the loss of Coiled-Coil or NHL domain reduced or nearly abolished the binding of *TRIM71* to LIN28B (Appendix Fig S3), which correlated with the inability of Coiled-Coil or NHL-deficient *TRIM71* to upregulate the expression of the *let-7* target *Hmga2* in cochlear organoids (Fig EV3B). However, TaqMan-based analysis of mature *let-7a*, *let-7d*, *let-7g* and *let-7i* miRNA expression in control and *TRIM71*-expressing organoids revealed no significant changes (Fig EV3C). By contrast, mature *let-7a*, *let-7d*, *let-7g*, and *let-7i* miRNAs were near absent in organoids in which we overexpressed human *LIN28B* using a doxycycline-inducible transgenic mouse model (Fig EV3D). *TRIM71* also destabilizes and inactivates *let-7* miRNAs by inhibiting the expression of Argonaute 2 (AGO2; Rybak et al, 2009; Liu et al, 2021). AGO2 is a critical component of

**Figure 4. *TRIM71* activates genes linked to self-renewal and de-differentiation in cochlear supporting cells/Kölliker's cells.**

- A–C Cochlear epithelial cells isolated from P5 wild-type mice were transduced with control (Ctrl) or *TRIM71*-expressing lentivirus and bulk RNA sequencing was used to analyze differential gene expression after 10 days of expansion. (A) Volcano plot of RNA-seq data. Plotted is the beta-value (x-axis) versus  $-\log_{10}$   $q$ -value (y-axis). Transcripts that are significantly upregulated in response to *TRIM71* expression are marked in red circles, and transcripts that are significantly downregulated are marked in blue circles. (B) Biological processes/pathways associated with *TRIM71*-upregulated genes ranked by  $P$  value. (C) Biological processes/pathways associated with *TRIM71*-downregulated genes ranked by  $P$  value.
- D Venn diagram showing the intersection among *TRIM71*-upregulated genes, predicted *let-7* target genes, and LIN28B + FST-upregulated genes.
- E RT-qPCR-based analysis of *Bmp4*, *Id1*, *Id2*, *Id3* expression in P5 control, *TRIM71*-expressing or  $\Delta$ NHL expressing cochlear organoids after 10 days of expansion. Plotted are individual data points, representing the average value per animal and treatment, and mean  $\pm$  SD of biological replicates ( $n = 3$ , two independent experiments). One-way ANOVA with Tukey's correction was used to calculate  $P$  values. \* $P \leq 0.05$ , \*\* $P < 0.01$ , \*\*\* $P < 0.001$  and \*\*\*\* $P < 0.0001$ .
- F Immunoblots showing LIN28B, AGO2, HMGA2, P-SMAD1/5/9 and  $\beta$ -actin protein levels in P5 control, *TRIM71* and  $\Delta$ NHL expressing cochlear organoids at 10 days of expansion. Note  $\beta$ -actin was used to normalize protein levels.

Source data are available online for this figure.



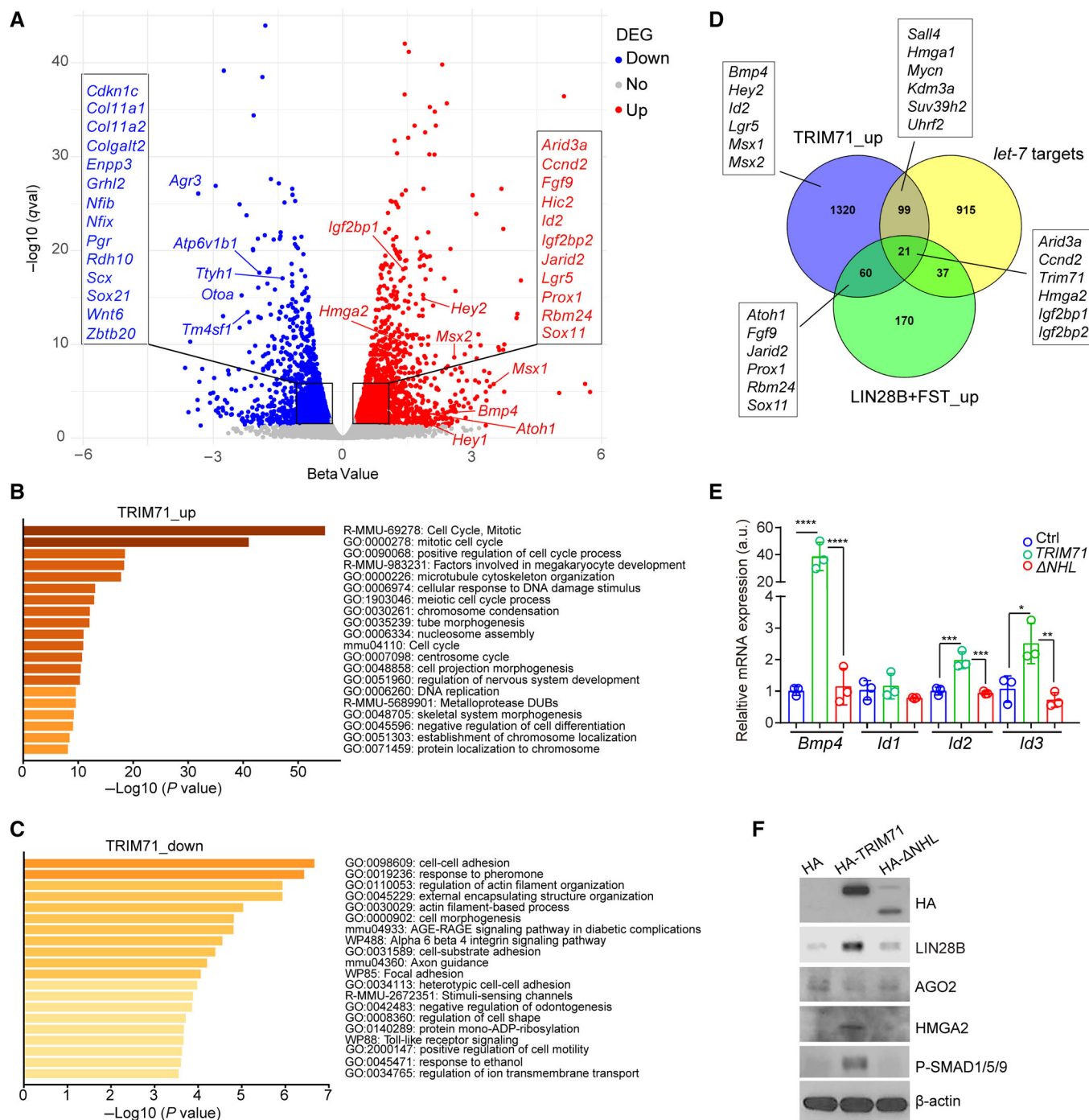


Figure 4.

the RNA-Induced Silencing Complex (RISC). However, western blot analysis of AGO2 protein levels in control cultures and cultures that expressed full-length TRIM71 or an NHL-deficient form of TRIM71 protein revealed no significant changes in AGO2 expression across these conditions (Fig 4F). In sum, TRIM71 reactivation in cochlear supporting cells/Kölliker’s cells does not reduce the expression of mature *let-7* miRNAs, nor does it reduce AGO2 expression, suggesting that TRIM71 increases the abundance of *let-7* targets through directly binding and stabilizing their mRNA transcripts.

**TRIM71 promotes the de-differentiation of cochlear supporting cells/Kölliker’s cells**

The observed upregulation of progenitor cell genes and the downregulation of supporting cell/Kölliker’s cell genes suggest that re-expression of *TRIM71* may reprogram supporting cells/Kölliker’s cells into progenitor-like cells. To gain further insights, we used immunostaining to analyze the changes in supporting cell and progenitor cell-specific gene expression on a cellular level. To be

able to identify differentiated/de-differentiated supporting cells/Kölliker's cells, we co-stained organoids for the Notch ligand Jagged1 (JAG1), which is selectively expressed in cochlear supporting cells, Kölliker's cells, and their precursors (Morrison *et al*, 1999). As a progenitor cell-specific protein, we selected the pro-sensory cell protein HMGA2, which at stage P5 is near undetectable in cochlear supporting cells and Kölliker's cells (Li *et al*, 2022). Our analysis revealed that in control organoids, less than 5% of JAG1<sup>+</sup> mCherry<sup>+</sup> cells expressed HMGA2, while in *TRIM71*-expressing organoids, more than 50% of JAG1<sup>+</sup> mCherry<sup>+</sup> cells expressed HMGA2, (Fig 5A

and B). Conversely, in control organoids, 90% of JAG1<sup>+</sup> mCherry<sup>+</sup> cells also expressed the supporting cell-specific protein S100A1, while in *TRIM71*-expressing organoids, less than 30% of JAG1<sup>+</sup> mCherry<sup>+</sup> cells expressed S100A1 (Fig 5C and D). Potential candidates for driving *TRIM71*-induced changes in supporting cell-specific gene expression are the pro-differentiation transcription factors NFIB and ZBTB20 (Chen *et al*, 2017; Medeiros de Araújo *et al*, 2021). Immunostaining revealed that in the early postnatal cochlea, NFIB protein is broadly expressed in supporting cells and surrounding non-sensory epithelial cells including Kölliker's cells

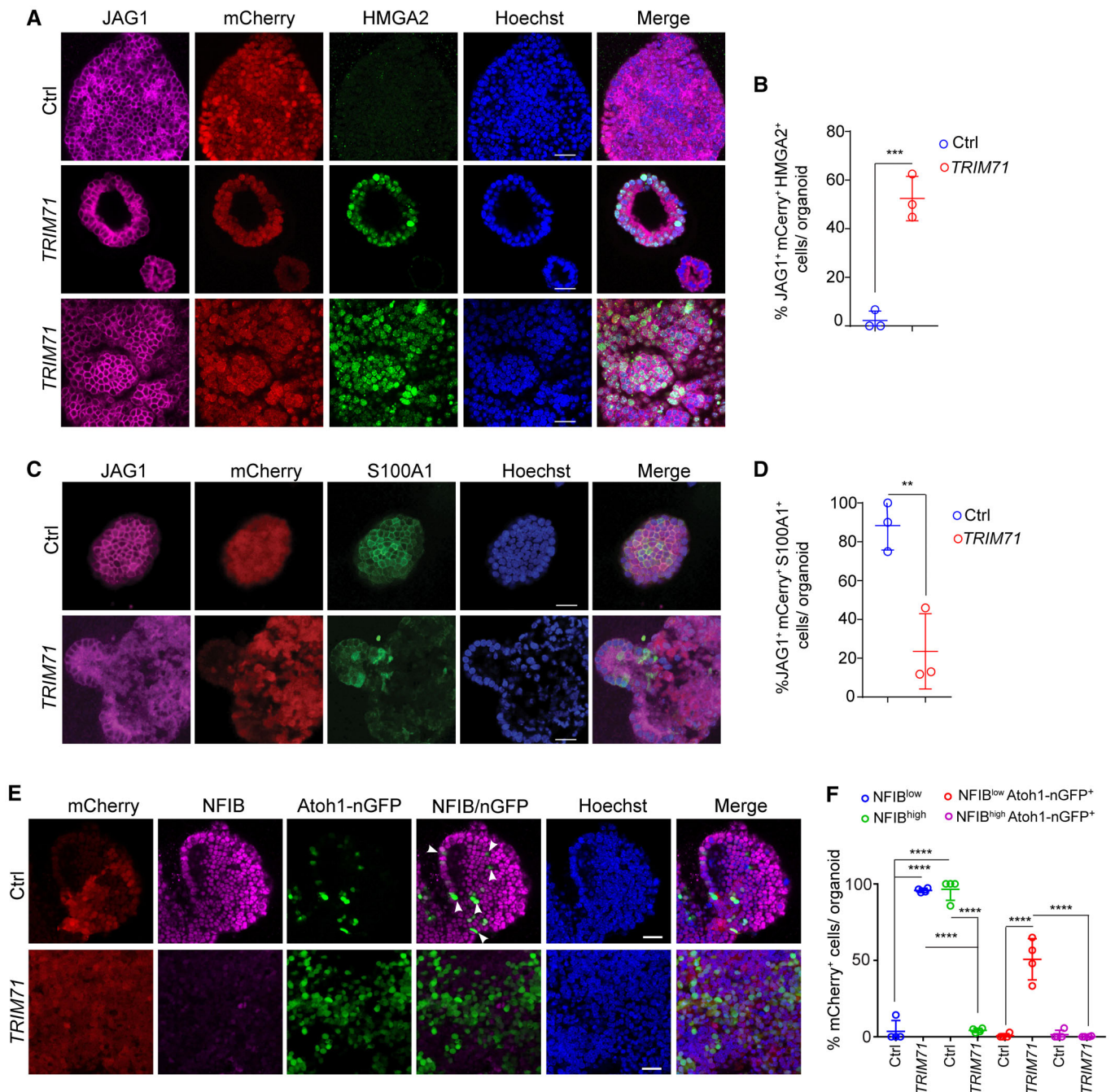


Figure 5.

**Figure 5. TRIM71 promotes de-differentiation of cochlear supporting cells/Kölliker's cells.**

- Cochlear epithelial cells isolated from P5 wild type (A–D) or *Atoh1*-nGFP transgenic mice (E, F) were transduced with control (Ctrl) or *TRIM71*-expressing lentivirus and expanded as organoids. MCherry (red) marks transduced cells. Hoechst staining (blue) labels cell nuclei.
- A High-power single-plane confocal images of control (Ctrl) and *TRIM71*-expressing organoids immuno-stained for progenitor/supporting cell marker JAG1 (magenta) and progenitor cell marker HMGA2 (green) after 10 days of expansion. Scale bars = 25  $\mu$ m.
- B Quantification of JAG1<sup>+</sup> mCherry<sup>+</sup> HMGA2<sup>+</sup> cells per organoid in (A) ( $n = 3$ , two independent experiments). A two-tailed, unpaired *t* test was used to calculate *P* values. \*\*\**P* < 0.001.
- C High-power confocal images of control (Ctrl) or *TRIM71*-expressing organoids immuno-stained for progenitor cell/supporting cell marker JAG1 (magenta) and supporting cell marker S100A1 (green) after 10 days of expansion. Scale bars = 25  $\mu$ m.
- D Quantification of JAG1<sup>+</sup> mCherry<sup>+</sup> S100A1<sup>+</sup> cells per organoid in (C) ( $n = 3$ , two independent experiments). A two-tailed, unpaired *t* test was used to calculate *P* values. \*\**P* < 0.01.
- E High-power, single-plane confocal images of control (Ctrl) or *TRIM71*-expressing organoids immuno-stained for transcription factor NFIB (magenta) after 2 days of differentiation. *Atoh1*-nGFP (green) marks nascent hair cells. White arrowheads mark *Atoh1*-GFP<sup>+</sup> cells with low NFIB expression (NFIB<sup>low</sup>). Scale bars = 25  $\mu$ m.
- F Quantification of NFIB<sup>low</sup>, NFIB<sup>high</sup>, NFIB<sup>low</sup>*Atoh1*-nGFP<sup>+</sup>, NFIB<sup>high</sup> *Atoh1*-nGFP<sup>+</sup> cells in control (Ctrl) and *TRIM71*-expressing organoids ( $n = 4$ , two independent experiments). Two-way ANOVA with Tukey's correction was used to calculate *P* values. \*\*\*\**P* < 0.0001.

Data information: Plotted are individual data points, representing the average value per animal and treatment, and mean  $\pm$  SD of biological replicates. Source data are available online for this figure.

(Fig EV4A), while ZBTB20 protein is expressed in supporting cells and lateral cochlear epithelial cells (Fig EV4B). Analysis of NFIB and ZBTB20 protein expression in differentiating cochlear organoids revealed that nearly 100% of *TRIM71*-expressing cells expressed little to no NFIB or ZBTB20, which we categorized as NFIB<sup>low</sup> cells (Fig 5E and F) and ZBTB20<sup>low</sup> cells, respectively (Fig EV4C and D). By contrast, in control organoids, high NFIB expression (NFIB<sup>high</sup>) was observed in close to 100% of cells (Fig 5E and F) and high ZBTB20 expression (ZBTB20<sup>high</sup>) in 60% of cells, which matched the narrower pattern of cochlear ZBTB20 expression observed *in vivo* (Fig EV4B). Furthermore, our analysis revealed that NFIB or ZBTB20 expression is negatively correlated with hair cell-fate induction, and only cells with no or low NFIB or ZBTB20 expression coexpressed *Atoh1*-nGFP (Figs 5E and F, and EV4C and D).

### TRIM71 and LIN28B are equally potent enhancers of supporting cell plasticity

We have previously shown that transgenic overexpression of human *LIN28B* (in the presence of FST or TGFBR inhibitor 616452) restores the hair cell-forming potential of P5 cochlear supporting cells/Kölliker's cells (Li & Doetzlhofer, 2020; Li et al, 2022). To be able to compare *TRIM71*'s and *LIN28B*'s ability in promoting hair cell formation, we transduced cochlear epithelial cells from stage P5 *Atoh1*-nGFP transgenic mice with lentiviral particles that expressed only *mCherry* (control) or coexpressed *mCherry* with either *TRIM71*, or *Lin28b*, or both (Figs 6A and B, and EV5A). We found that *TRIM71* and *Lin28b* coexpression increased the colony-forming efficiency compared to *TRIM71* or *Lin28b* alone (Fig 6C). By contrast, organoid diameter was increased by coexpression of *TRIM71* and *Lin28b* to a similar extent than observed by *TRIM71* or *Lin28b* alone (Fig 6D).

After 2 days of differentiation, more than 10% of *mCherry*<sup>+</sup> organoids in *TRIM71* or *Lin28b*-expressing cultures contained clusters of *Atoh1*-nGFP<sup>+</sup> cells, while control cultures lacked *Atoh1*-GFP<sup>+</sup> cell clusters. Moreover, we found that in cultures that were transduced with both *TRIM71* and *Lin28b*-expressing viral particles, about 25% of *mCherry*<sup>+</sup> organoids contained *Atoh1*-GFP<sup>+</sup> cells (Fig 6B and E). To compare the effects of *TRIM71* and/or *Lin28b* expression on supporting cell reprogramming, we analyzed *Hmga2*, *Nfib*, and

*Zbtb20* mRNA abundance using RT-qPCR. Our analysis revealed that individual expression of *TRIM71* or *Lin28b* decreased the expression of *Zbtb20* and *Nfib* by more than twofold, but *Zbtb20* and *Nfib* expression was not further decreased by the coexpression of *TRIM71* and *Lin28b* (Fig 6F). Similar results were obtained by analyzing the expression of *Nfib* family members *Nfia*, *Nfic*, and *Nfix* (Fig EV5B). By contrast, the coexpression of *TRIM71* and *Lin28b* further increased *Hmga2* expression by twofold compared to *TRIM71* or *Lin28b* alone (Fig 6F). In sum, our analysis reveals that *TRIM71* and *LIN28B* are equally potent enhancers of supporting cell reprogramming, and their coexpression has a strong additive effect on organoid formation and hair cell production.

### LIN28B-TRIM71 target gene *Hmga2* is required for cell cycle reentry of supporting cells/Kölliker's cells and their ability to form hair cells

The *TRIM71* and *LIN28B*-regulated gene *Hmga2* encodes a chromatin architectural protein that functions to maintain self-renewal capacity (Vignali & Marracci, 2020). To address the function of *HMGA2* in hair cell regeneration, we first examined whether *Hmga2* is necessary for cell cycle reentry, cell propagation, and hair cell formation in cochlear organoid culture (Fig 7A). To disrupt *Hmga2* gene function, we transduced cochlear epithelial cells from stage P2 mice with lentivirus that expressed a short-hairpin RNA (shRNA) targeting endogenous *Hmga2* (Winslow et al, 2011). Control cultures were transduced with lentivirus expressing a short-hairpin RNA with a scrambled (scr) sequence. After 8 days of expansion, we found that *Hmga2*-knockdown cultures contained on average fourfold fewer organoids than control cultures (Fig 7B). The average organoid size in *Hmga2*-knockdown cultures was, while mildly reduced, not significantly different from control cultures (Fig 7C). RT-qPCR confirmed the reduction in *Hmga2* expression in *Hmga2*-knockdown cultures and revealed a significant reduction in the expression of *Trim71* and *Atoh1* compared to control cultures (Fig 7D), indicating defects in reprogramming and hair cell-fate induction, respectively. We next analyzed the ability of organoid cells to differentiate into hair cells in *Hmga2* knockdown and control organoid cultures. We found that the percentage of *Atoh1*-GFP<sup>+</sup> organoids in *Hmga2* knockdown cultures was significantly reduced compared to control cultures, indicating that *Hmga2* is required for



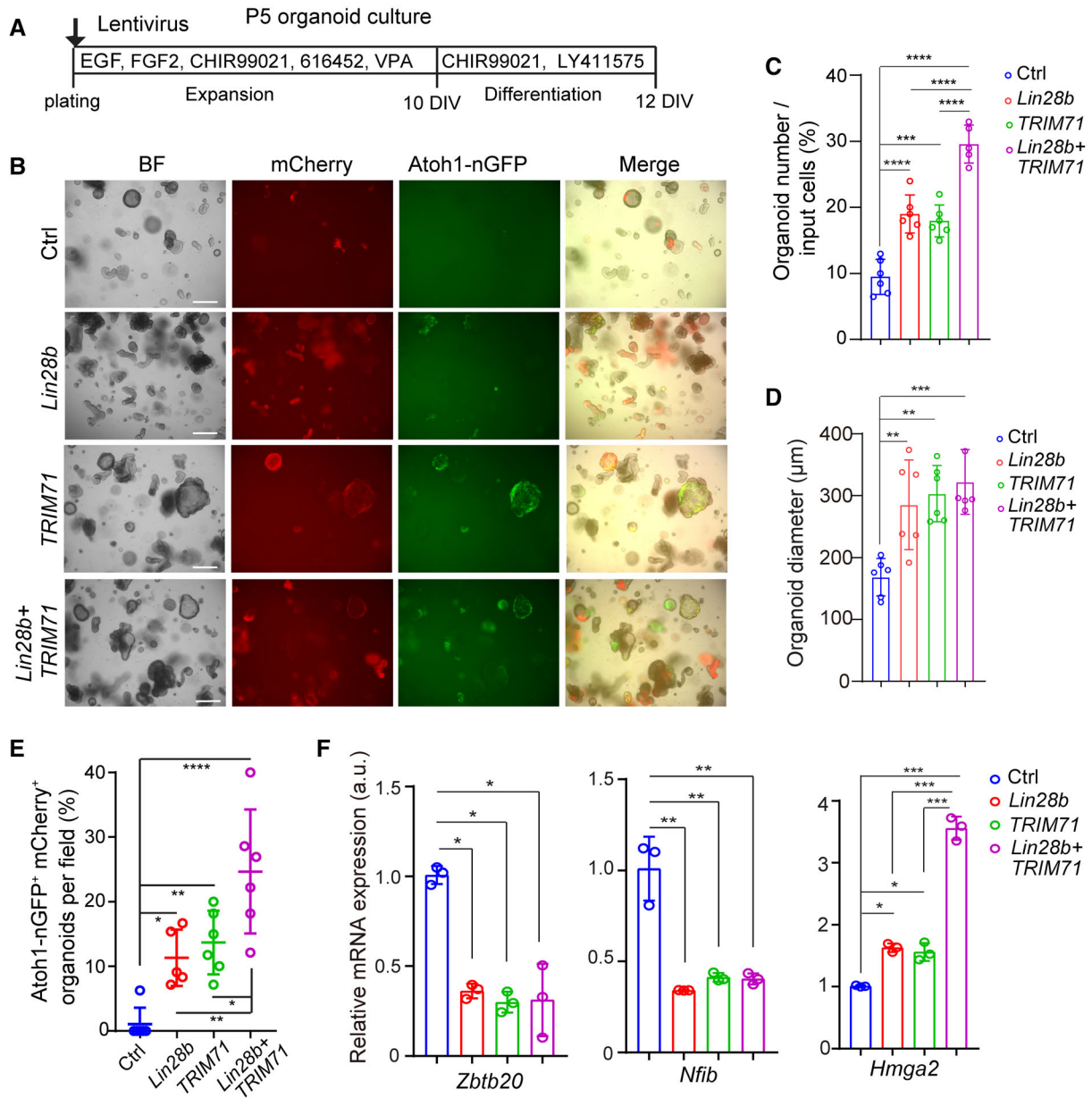


**Figure 6. LIN28B enhances TRIM71's positive effect on cell cycle reentry and hair cell formation.**

A Experimental scheme. Cochlear epithelial cells from P5 Atoh1-GFP transgenic mice were transduced with control (Ctrl) lentivirus, or lentivirus that expressed mouse *Lin28b* or human *TRIM71* or co-transduced with both (*Lin28b* + *TRIM71*) and cultured as indicated.

B Bright-field (BF) and red and green fluorescent images of organoid cultures at 2 days of differentiation. MCherry (red) marks transduced cells and Atoh1-nGFP (green) marks nascent hair cells. Scale bars = 400  $\mu$ m.

C Colony forming efficiency in (B) ( $n = 5$  for *Lin28b* + *TRIM71* group,  $n = 6$  for all the other groups, two independent experiments). One-way ANOVA with Tukey's correction was used to calculate  $P$  values. \*\*\*\* $P < 0.0001$ .

D Organoid diameter in (B) ( $n = 5$  for *Lin28b* + *TRIM71* group,  $n = 6$  for all the other groups; two independent experiments). One-way ANOVA with Tukey's correction was used to calculate  $P$  values. \*\* $P < 0.01$ , \*\*\* $P < 0.001$ .

E Percentage of mCherry<sup>+</sup>Atoh1-nGFP<sup>+</sup> organoids in (B) ( $n = 5$  for *Lin28b* group,  $n = 6$  for all the other groups; two independent experiments). One-way ANOVA with Tukey's correction was used to calculate  $P$  values. \* $P \leq 0.05$ , \*\* $P < 0.01$  and \*\*\*\* $P < 0.0001$ .

F RT-qPCR-analysis of progenitor cell (*Hmga2*) and supporting cell-specific (*Zbtb20*, *Nfib*) gene expression in control, *Lin28b*, *TRIM71* or *Lin28b* + *TRIM71*-expressing organoids after 10 days of expansion ( $n = 3$ , two independent experiments). One-way ANOVA with Tukey's correction was used to calculate  $P$  values. \* $P \leq 0.05$ , \*\* $P < 0.01$  and \*\*\*\* $P < 0.0001$ .

Data information: Plotted are individual data points, representing the average value per animal and treatment, and mean  $\pm$  SD of biological replicates.

Source data are available online for this figure.



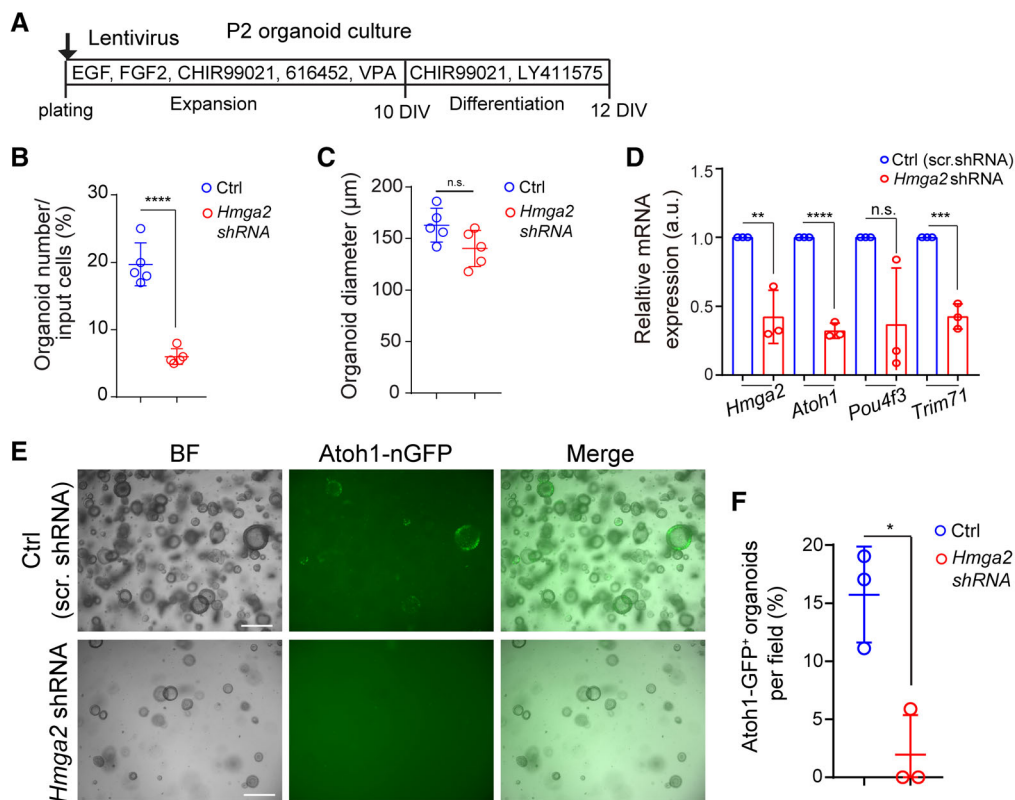


**Figure 7. LIN28B-TRIM71 target *Hmga2* is necessary for cochlear supporting cell reentry and subsequent hair cell formation.**

A Experimental scheme. Cochlear epithelial cells from P2 *Atoh1*-GFP transgenic mice were transduced with lentivirus expressing scrambled shRNA (control, Ctrl) or lentivirus expressing shRNA targeting endogenous *Hmga2*, and were cultured as indicated.

B Colony forming efficiency in *Hmga2* knockdown and control organoid cultures after 8 days of expansion ( $n = 5$ , two independent experiments). A two-tailed, unpaired t test was used to calculate  $P$  values. \*\*\*\* $P < 0.0001$ .

C Organoid diameter in *Hmga2* knockdown and control organoid cultures after 8 days of expansion ( $n = 5$ , two independent experiments). A two-tailed, unpaired t test was used to calculate  $P$  values. n.s., not significant.

D RT-qPCR analysis of hair cell (*Atoh1* and *Pou4f3*) and progenitor cell-specific (*Trim71*) gene expression in *Hmga2* knockdown and control cultures. *Hmga2* expression was analyzed to confirm knockdown. Plotted are the fold difference between the control and *Hmga2* shRNA groups and mean  $\pm$  SD ( $n = 3$ , biological replicates; two independent experiments). A two-tailed, unpaired t test was used to calculate  $P$  values. \*\* $P < 0.01$ , \*\*\* $P < 0.001$  and \*\*\*\* $P < 0.0001$ .

E Low power bright-field (BF) and green fluorescent images (*Atoh1*-nGFP) of *Hmga2* shRNA knockdown and control organoid cultures after 2 days of differentiation. Scale bars = 400  $\mu$ m.

F Quantification of *Atoh1*-nGFP<sup>+</sup> organoids in (E) ( $n = 3$ , two independent experiments). A two-tailed, unpaired t test was used to calculate  $P$  values. \* $P \leq 0.05$ .

Data information: (B, C, F) Plotted are individual data points, representing the average value per animal and treatment, and mean  $\pm$  SD of biological replicates. Source data are available online for this figure.

hair cell formation (Fig 7E and F). We next analyzed whether lentiviral expression of human *HMGA2* restores the capacity of stage P5 cochlear epithelial cells to form and grow large hair cell-containing organoids (Appendix Fig S4A). Our analysis of organoid formation efficiency and organoid growth revealed no differences between control and *HMGA2*-overexpressing organoid cultures (Appendix Fig S4B and C), indicating that *HMGA2* overexpression is not sufficient to boost the mitotic capacity of P5 cochlear supporting cells/Kölliker's cells. Next, we analyzed the hair cell-forming capacity of control and *HMGA2*-overexpressing organoid cultures. We found that both control and *HMGA2*-expressing cultures lacked *Atoh1*-nGFP<sup>+</sup> organoids after 2 days of differentiation, indicating that *HMGA2* overexpression is not sufficient to enhance the hair cell regenerative capacity of P5 cochlear supporting cells/Kölliker's cells (Appendix Fig S4D and E). In sum, our findings indicate that *Hmga2*

function is required for cell cycle reentry (organoid formation) and hair cell formation at neonatal stages. However, *HMGA2* overexpression is not sufficient for restoring the capacity of supporting cells/Kölliker's cells to reenter the cell cycle and form hair cells at later postnatal stages.

## Discussion

The loss of cochlear hair cells due to loud noise, viral infection, exposure to ototoxic substances, or aging, to name only a few, is permanent, resulting in hearing deficits and deafness. Recent studies in mice have shown that immature cochlear supporting cells do have some latent capacity for hair cell regeneration (reviewed in Zhang *et al*, 2020). However, their ability to form hair cells rapidly

declines as cochlear supporting cells undergo maturation. Direct reprogramming strategies such as expressing the hair cell–competence factor ATOH1 by itself (Kelly *et al*, 2012; Liu *et al*, 2012) or in combination with other hair cell–specific transcription factors (e.g. POU4F3, GFI1; Walters *et al*, 2017; Chen *et al*, 2021; Sun *et al*, 2021) are highly successful in converting cochlear supporting cells into hair cells at neonatal stages, but thus far these strategies had no or only very limited success at later stages (Kelly *et al*, 2012; Liu *et al*, 2012; Lee *et al*, 2020; Sun *et al*, 2021).

We recently showed that rising levels of *let-7* miRNAs during cochlear maturation are a considerable barrier for hair cell regeneration and found that the mitotic and hair cell regenerative potential of cochlear supporting cells can be enhanced by overexpression of the RNA-binding protein and *let-7* antagonist LIN28B (Li & Doetzlhofer, 2020; Li *et al*, 2022). Here, using an organoid culture platform, we find that the LIN28B/*let-7* target gene *Trim71* is essential for pro-sensory cell self-renewal and hair formation at embryonic stages, and we show that the presence of TRIM71 at postnatal stages enhances the mitotic and hair cell regenerative potential of cochlear supporting cells (and Kölliker's cells) to a similar extent as LIN28B. The strong additive effect on cell cycle reentry and hair cell formation that is observed when *TRIM71* and *Lin28b* genes are coexpressed indicates a strong, but non-comprehensive functional overlap between them, but also non-redundant contributions, which is consistent with the findings of our RNA-seq data analysis.

TRIM71 is a potent posttranscriptional regulator, having a dual function as a ubiquitin ligase (Rybak *et al*, 2009) and RNA-binding protein (Loedige *et al*, 2013). Previous studies suggested that TRIM71-mediated ubiquitination of the tumor suppressor protein p53 (Nguyen *et al*, 2017) and the FGF regulatory protein SHCBP1 (Chen *et al*, 2012) may be critical for maintaining embryonic stem cells and neural progenitor cells in an undifferentiated, proliferative state. However, our data indicate that TRIM71's ubiquitination activity is dispensable for enhancing the mitotic and regenerative potential of cochlear supporting cells/Kölliker's cells. We found that TRIM71 mutant protein that lacked the RING domain ( $\Delta$ RING), which is critical for TRIM71's ubiquitin ligase activity, enhanced the mitotic and hair cell regenerative capacity of cochlear supporting cells to a similar extent as wild-type TRIM71. By contrast, TRIM71 mutant protein that lacked the NHL domain, which is essential for RNA binding, failed to boost the mitotic and regenerative potential of cochlear supporting cells/Kölliker's cells. The importance of TRIM71's NHL domain for the regulation of progenitor cell proliferation and differentiation is further highlighted by a recent study that revealed that mice homozygous for a point mutation in TRIM71's NHL domain (R608H) have severe brain defects due to reduced cell proliferation and premature neuro-epithelial cell differentiation (Duy *et al*, 2022). Likewise, the direct binding of TRIM71 to the mRNAs of the cell cycle inhibitor p21 (CDKN1A) and the pro-differentiation factor EGR1 has been shown to be essential for promoting proliferation and cell reprogramming, respectively (Worringer *et al*, 2014; Torres-Fernandez *et al*, 2019).

Recent studies revealed that TRIM71 interferes with the expression and function of mature *let-7* miRNAs through enhancing LIN28A and LIN28B-mediated repression of *let-7* biogenesis (Torres Fernández *et al*, 2021) and through limiting the expression of AGO2, an essential component of miRNA-mediated gene silencing (Liu *et al*, 2021). Indeed, our transcriptomic profiling revealed that

many of the upregulated genes that were shared between TRIM71 and LIN28B are known or predicted targets of *let-7*-mediated gene silencing. However, further analysis revealed that TRIM71 did not reduce the expression of mature *let-7* miRNAs in cochlear organoids, nor did the presence of TRIM71 reduce AGO2 protein expression in cochlear organoids, suggesting that TRIM71 may increase the expression of *let-7* target genes by directly binding to their mRNA and stabilizing their transcript.

How does TRIM71 enhance the mitotic and hair cell-forming potential of cochlear supporting cells? Based on our data, we propose that TRIM71 reprograms cochlear supporting cells into progenitor-like cells. Supporting the idea of de-differentiation, we find that a subset of supporting cell-specific genes is rapidly downregulated in the presence of TRIM71 or LIN28B. This includes the transcription factor ZBTB20 and members of the NFI family of transcription factors (NFIA, B, C, X). ZBTB20 and NFI transcription factors function as pro-differentiation factors in glial cell types, (Chen *et al*, 2017; Medeiros de Araújo *et al*, 2021), and it is tantalizing to speculate that the TRIM71 or LIN28B-induced downregulation of *Nfia,b,c,x* and *Zbtb20* expression may be a key step in priming cochlear supporting cells for hair cell–fate induction. The notion that NFI factors and ZBTB20 may interfere with hair cell–fate induction is supported by our finding that high NFIB and ZBTB20 protein expression is negatively correlated with hair cell–fate induction (Atoh1-GFP expression) in cochlear supporting cells. Future studies are warranted to address the role of ZBTB20 and NFI-type transcription factors in cochlear supporting cell differentiation and plasticity.

Among the genes that were upregulated by the expression of *TRIM71* or *Lin28b* or both was the *let-7* target gene *Hmga2*. HMGA2, a member of the high-mobility group (HMG) protein family, is highly expressed in fetal and adult stem cells where it acts to maintain self-renewal potential (Nishino *et al*, 2008; Copley *et al*, 2013). In the developing cochlea, high *Hmga2* expression is confined to pro-sensory cells (Golden *et al*, 2015), and we recently found that at neonatal stages, HMGA2 expression is upregulated in apical cochlear supporting cells in response to hair cell damage, suggesting that *Hmga2* re-activation may be part of an endogenous regenerative response (Li *et al*, 2022). Indeed, our *Hmga2* knockdown experiments indicate that the presence of HMGA2 is essential for the ability of cochlear supporting cells to reenter the cell cycle and generate hair cells. How does HMGA2 facilitate cell cycle reentry? HMGA2 has been shown to disrupt the binding of the retinoblastoma protein (RB1) to the S-phase-specific transcription factor E2F1, leading to the activation of E2F1, a step essential for cell cycle reentry (Fedele *et al*, 2006). Furthermore, our data suggest the existence of a positive feedback loop between HMGA2 and TRIM71. We show that *Hmga2* knockdown in cochlear organoids reduces *Trim71* expression. The 3'UTR of *Hmga2* mRNA contains multiple *let-7* binding sites (Mayr *et al*, 2007), and *Hmga2* knockdown would free up *let-7* miRNAs to target *Trim71* mRNA. Alternatively, HMGA2 may act as a transcriptional co-activator for *Trim71*. Surprisingly, HMGA2 overexpression fails to enhance the mitotic and hair cell-forming potential of stage P5 cochlear supporting cells. Why does HMGA2 overexpression fail to boost supporting cell plasticity? HMGA2 and other HMG proteins do not directly regulate transcriptional activity, but rather control gene expression by changing chromatin structure and acting as co-factor for transcription factors (Vignali & Marracci, 2020). Thus, it is likely that changes in transcription

factors expression/activity at the onset of cochlear maturation may limit HMGA2's ability to enhance the regenerative potential of cochlear supporting cells.

TRIM71 and its downstream target HMGA2 are critical regulators of stem cell behavior (Nishino *et al*, 2008; Zhu *et al*, 2011; Mitschka *et al*, 2015), and both are known to enhance the reprogramming of adult somatic cells into induced pluripotent stem cells and neural stem cells (Worringer *et al*, 2014; Yu *et al*, 2015). However, TRIM71's role in cell/tissue regeneration is much less well understood. In the nematode *C. elegans*, LIN-41 (TRIM71 orthologue) acts as an axon regeneration-promoting factor in young anterior ventral microtubule (AVM) neurons, whereas in older AVM neurons, high levels of *let-7* inhibit regeneration through repression of LIN-41 (Zou *et al*, 2013). Our work

reveals that TRIM71's ability to stimulate regeneration is evolutionarily conserved and thus lays the foundation for further studies investigating the role of the *let-7*-TRIM71 axis in cell/tissue regeneration in mammalian and non-mammalian vertebrates. Furthermore, it will be of interest to determine whether TRIM71 facilitates cell regeneration in other sensory tissues such as the inner ear vestibular organs and the retina.

A limitation of our study is that we have yet to show whether TRIM71 would be effective in reprogramming fully mature cochlear supporting (P12 and older) into hair cell progenitor-like cells and whether TRIM71 itself or in combination with LIN28B could bolster current regenerative strategies, such as ATOH1 activation, and promote cochlear hair cell formation *in vivo*, especially at adult stages in mammals.

## Materials and Methods

### Reagents and Tools table

| Antibodies                                   | Reference or Source         | Identifier or Catalog Number |
|--|-----------------------------|------------------------------|
| myosinVIIa rabbit polyclonal                 | Proteus Biosciences         | Cat. #25-6790                |
| SOX2 goat polyclonal                         | Santa Cruz                  | Cat. #sc-17320               |
| JAG1 goat polyclonal                         | Santa Cruz                  | Cat. #sc-6011                |
| HMGA2 rabbit monoclonal                      | Cell Signaling              | Cat. #8179                   |
| S100-alpha rabbit polyclonal                 | Abcam                       | Cat. #ab11428                |
| ZBTB20 rabbit polyclonal                     | Sigma                       | Cat. #HPA016815              |
| NFIB rabbit polyclonal                       | Sigma                       | Cat. #HPA003956              |
| donkey anti-rabbit IgG (H+L) Alexa Fluor 647 | ThermoFisher                | Cat. #A-31573                |
| donkey anti-rabbit IgG (H+L) Alexa Fluor 488 | ThermoFisher                | Cat. #A32790                 |
| donkey anti-goat IgG (H+L) Alexa Fluor 647   | ThermoFisher                | Cat. #A32849                 |
| donkey anti-goat IgG (H+L) Alexa Fluor 488   | ThermoFisher                | Cat. #A-11055                |
| Biotinylated donkey anti goat                | Jackson Immuno Research Lab | Cat. #705-065-147            |
| Streptavidin, Alexa Fluor 405                | Life Technologies           | Cat. #S32351                 |
| Hoechst 33258 solution                       | Sigma-Aldrich               | Cat. #94403                  |
| FLAG (M2) mouse monoclonal                   | Sigma                       | Cat. #F1804                  |
| LIN28B (mouse preferred) rabbit polyclonal   | Cell Signaling              | Cat. #5422                   |
| AGO2 rabbit monoclonal                       | Cell Signaling              | Cat. #2897                   |
| P-SMAD1/5/9 (D5B10) rabbit monoclonal        | Cell Signaling              | Cat. #13820                  |
| $\beta$ -actin mouse monoclonal              | Santa Cruz                  | Cat. #47778                  |
| HRP-conjugated donkey anti-mouse IgG         | Jackson Immuno Research     | Cat. #715-035-150            |
| HA (C29F4) rabbit monoclonal                 | Cell Signaling              | Cat. #3724                   |
| HRP-conjugated goat anti-rabbit IgG          | Jackson Immuno Research     | Cat. #111-035-003            |

| QPCR primers  |                                |                             |
|---------------|--------------------------------|-----------------------------|
| Gene          | Forward Primer                 | Reverse Primer              |
| <i>Ano1</i>   | TTC CCT CTG GCT CCA CTC TTC    | GGC ATC CAG GCG GAT CT      |
| <i>Atoh1</i>  | ATG CAC GGG CTG AAC CA         | TCG TTG TTG AAG GAC GGG ATA |
| <i>Bmp4</i>   | ACG TAG TCC CAA GCA TCA CC ACT | AGG GTC TGC ACA ATG GC      |
| <i>Ccnd2</i>  | GGG ATC CCT GTA CAC TCG AA     | TTG CAG GTA CGC ACA CTC TC  |
| <i>Cybrd1</i> | AGA CTG CCA TGG ACC TGG AA     | CCG GCA TGG ATG GAT TTC     |

Reagents and Tools table (continued)

| QPCR primers                  |  |                               |
|-------------------------------|--|-------------------------------|
| Gene                          | Forward Primer   | Reveres Primer                |
| <i>Fat3</i>                   | CAC AGC CCT TGA ATA CAG TGA  | TGC CTT TGC ATC TCC TTC CT    |
| <i>Fst</i>                    | GAA AAC CTA CCG CAA CGA ATG  | TCC GGC TGC TCT TTG CAT       |
| <i>Gfi1</i>                   | AGGAACGCAGCTTTGACTGT   | TGAGATCCACCTTCCTCTGG          |
| <i>Hmga2</i>                  | CAG AAG AAA GCA GAG ACC ATT GG   | TTG TTG TGG CCA TTT CCT AGG T |
| <i>Id1</i>                    | GAA CGT CCT GCT CTA CGA CAT G  | TGG GCA CCA GCT CCT TGA       |
| <i>Id2</i>                    | AAG GTG ACC AAG ATG GAA ATC CT   | CGA TCT GCA GGT CCA AGA TGT   |
| <i>Id3</i>                    | GAG CTC ACT CCG GAA CTT GTG  | CGG GTC AGT GGC AAA AGC       |
| <i>Lgr5</i>                   | CCC CAA TGC GTT TTC TAC GT   | GAA GGA CGA CAG GAG ATT GGA T |
| <i>Myo7a</i>                  | CCC CCT CTG AGA AGT TCG TTA A  | TGT GTC CGA GTT CCG TTG AC    |
| <i>Nfia</i>                   | GAG TCC AGG AGC AAT GAG G  | CCA TTT CAT CCT CCA CAG AC    |
| <i>Nfib</i>                   | GTG TTC AGC CAC ACC ACA TC   | GAG GAT TCT TGG CAG GAT CA    |
| <i>Nfic</i>                   | CCG GCA TGA GAA GGA CTC TAC  | TTC TTC ACC GGG GAT GAG ATG   |
| <i>Nfix</i>                   | AGG CTG ACA AGG TGT GGC  | CAC TGG GGC GAC TTG TAG AG    |
| <i>Pou4f3</i>                 | GCA CCA TCT GCA GGT TCG A  | CCG GCT TGA GAG CGA TCA T     |
| <i>Rpl19</i>                  | GGT CTG GTT GGA TCC CAA  | TGC CCG GGA ATG GAC AGT CA    |
| <i>S100a1</i>                 | TGG ATG TCC AGA AGG ATG CA   | CCG TTT TCA TCC AGT TCC TTC A |
| <i>Sox2</i>                   | CCA GCG CAT GGA CAG CTA  | GCT GCT CCT GCA TCA TGC T     |
| <i>Trim71</i>                 | ATC GGG AGT GTG AGC TGT TG   | GGC GTG AAC ATA ATG CCG TC    |
| <i>Zbtb20</i>                 | GGC ATC TGA GGA GAA TGA GA   | GTT GTG AAG GTT GAT GCT GTG   |
| <i>TRIM71</i>                 | CGAGGCATAAGAAAGCCCTGGA   | GCTTGTGAGGTTTTGCCGAC          |
| Genotyping primers            |  |                               |
| Mouse line                    | Primer sequence  | Product size                  |
| <i>Trim71<sup>fl/fl</sup></i> | LIN41-F-WT: GAA AGG AGG CTA GCC AAA GG<br>LIN41-R-KO: ATG CTG TAC GGT AGG AGT CTT CC                     | FL = 350 bp<br>WT = 250 bp    |
| <i>Col1a-TRE-LIN28B</i>       | CoIA: GCA CAG CAT TGC GGA CAT GC<br>CoIB: CCC TCC ATG TGT GAC CAA GG<br>CoIC: GCA GAA GCG CGG CCG TCT GG | WT = 300 bp<br>TG = 450 bp    |
| <i>Atoh1-nGFP</i>             | EGFP1: CGA AGG CTA CGT CCA GGA GCG CAC<br>EGFP2: GCA CGG GGC CGT CGC CGA TGG GGG TGT                     | TG = 300 bp                   |
| <i>TetO-cre</i>               | F: GCC TGC ATT ACC GGT CGA TGC AAC GA<br>R: GTG GCA GAT GGC GCG GCA ACA CCA TT                           | TG = 700 bp                   |

## Methods and Protocols

### Mouse breeding and genotyping

All experiments and procedures were approved by the Johns Hopkins University Institutional Animal Care and Use Committees protocol, and all experiments and procedures adhered to National Institutes of Health–approved standards. The *Atoh1-nGFP* transgenic (tg) (MGI:3703598) mice were provided by Jane Johnson, University of Texas Southwestern Medical Center, Dallas, TX (Lumpkin et al, 2003). The *Col1a1-TRE-LIN28B* (MGI:5294612) mice were provided by George Q. Daley, Children’s Hospital, Boston, MA (Zhu et al, 2011). *Trim71<sup>fl/fl</sup>* mice were provided by Waldemar Kolanus (LIMES Institute, Universität Bonn, Germany; Mitschka et al, 2015). *TetO-cre* (No. 006234) and *R26<sup>rtTA\*M2</sup>* (No. 006965) mice were purchased from Jackson Laboratories (Bar Harbor, ME).

We crossed *TetO-cre tg*; *Trim71<sup>fl/fl</sup>* males/ females with *Trim71<sup>fl/fl</sup>*; *R26<sup>rtTA\*M2/rtTA\*M2</sup>* males/ females to obtain *Trim71 KO (TetO-cre tg*; *R26<sup>rtTA\*M2/+</sup>*; *Trim71<sup>fl/fl</sup>*) and control littermates (*R26<sup>rtTA\*M2/+</sup>*; *Trim71<sup>fl/fl</sup>*). To induce Cre expression, doxycycline (dox) was delivered to time-mated females via *ad libitum* access to feed containing 2 g/kg dox. Mice were genotyped by PCR as previously published. Genotyping primers are listed in the [Reagents and Tools table](#). Mice of both sexes were used in this study. Embryonic development was considered as E0.5 on the day a mating plug was observed.

### Lentiviral vectors and production

Expression plasmids for full-length and mutant TRIM71 ( $\Delta$ RING,  $\Delta$ Coiled-coil, and  $\Delta$ NHL) proteins were generated by subcloning HA-tagged human *TRIM71* and its mutant variants sequences from



*pMXS-hs-3xHA-TRIM71* (Addgene, no. 52717), *pMXS-hs-3xHA-deltaRING-TRIM71* (Addgene, no. 52718), *pMXS-hs-3xHA-deltaCoiled Coil-TRIM71* (Addgene, no. 52720) and *pMXS-hs-3xHA-delta6xNHL-TRIM71* (Addgene, no. 52722) into *pCDH-EF1a-eFFly-T2A-mCherry* (Addgene, no. 104833) replacing eFFly using restriction enzymes XbaI (NEB, no. R0145) and EagI-HF (NEB, no. R3505). TRIM71-R608H expression plasmid was generated by cloning DNA fragment-R608H (Integrated DNA Technology; Appendix Table S1) into *pCDH-EF1a-3xHA-TRIM71-T2A-mCherry* plasmid using SmaI (NEB, no. R0141) and EcoRI-HF (NEB, no. R3101). TRIM71-R796H expression plasmid was generated by cloning DNA fragment-R796H (Integrated DNA Technology; Appendix Table S1) into *pCDH-EF1a-3xHA-TRIM71-T2A-mCherry* using EcoRI-HF and EagI-HF. TRIM71-R608H + R796H expression plasmid was generated by cloning DNA fragment-R608H into *pCDH-EF1a-3xHA-TRIM71-(R796H)-T2A-mCherry* using Sma I and EcoRI-HF. Lentiviral control plasmid was generated by replacing the eFFly in *pCDH-EF1a-eFFly-T2A-mCherry* with a 3xHA sequence using restriction enzymes XbaI and BamHI-HF (NEB, no. R3136). Expression plasmid for CRE protein was generated by subcloning Cre from *LentiCRISPRv2Cre* (Addgene, no. 82415) into *pCDH-EF1a-eFFly-T2A-mCherry* (Addgene, no. 104833) replacing eFFly using restriction enzymes XbaI and EagI-HF. The *pFUWFLAG-Lin28b-F2A-mCherry* construct expressing mouse *Lin28b* under the control of human ubiquitin C promoter was previously described (Golden et al, 2015). Lentiviral constructs for HMGA2 overexpression were obtained by subcloning human *HMGA2* from *pMXS-hs-HMGA2* (Addgene, no. 52727) into *pCDH-EF1a-eFFly-mCherry* replacing eFFly using restriction enzymes Xba I and BamH I-HF. Lentiviral *shHmga2* construct was purchased from Addgene (no. 32399). Lentiviral packaging was conducted as previously described (Li et al, 2022).

#### Adeno-associated viral (AAV) vectors and production

The *pAAV-EF1a-3xHA-TRIM71-WPREs* and *pAAV-nEF1a-3xHA-WPREs* vectors were produced by subcloning 3xHA-tagged human *TRIM71* and 3xHA-only into *pAAV-EF1a-WPRE* construct. AAV particles were produced with AAV packaging plasmid that expressed the ancestral capsid Anc80L65 at a titer of  $5 \times 10^{12}$  viral particles per ml by Biohippo Inc.

#### Organoid culture

Cochlear organoid cultures were conducted as previously described (Li & Doetzlhofer, 2020). Briefly, cochlear epithelia were enzymatically isolated from stage P2 or P5 mice, reduced to single cells, and for lentiviral infection, cells were mixed and centrifuged with lentiviral particles at 600 g for 30 min. Otherwise, cells were immediately resuspended in expansion medium [DMEM/F12 (Corning, no. 10-092-CV), N-2 supplement (1 $\times$ , ThermoFisher, no. 17502048), B-27 supplement (1 $\times$ , ThermoFisher, no. 12587010), EGF (50 ng/ml, Sigma-Aldrich, no. SRP3196), FGF2 (50 ng/ml, ThermoFisher, no. PHG0264), CHIR99021 (3  $\mu$ M, Sigma-Aldrich, no. SML1046), VPA (1 mM, Sigma-Aldrich, no. P4543), 616,452 (2  $\mu$ M, Sigma-Aldrich, no. 446859-33-2), and penicillin (100 U/ml, Sigma-Aldrich, no. P3032)] mixed 1:1 with Matrigel (Corning, no. 356231). Organoids were expanded for up to 10 days. To induce hair cell formation, organoids were cultured in differentiation medium [DMEM/F12, N2 (1 $\times$ ), B27 (1 $\times$ ), CHIR99021 (3  $\mu$ M), and LY411575 (5  $\mu$ M, Sigma-Aldrich, no. SML0506)].

#### Cochlear explant culture

Cochleae were isolated from stage P2 wild-type mice and dissected in PBS with fungizone (250 ng/ml, ThermoFisher, A9528), ampicillin (10  $\mu$ g/ml, Sigma Aldrich, no. A5354). After removing the lateral wall, roof, and spiral ganglion, the remaining cochlear sensory epithelium was transferred onto SPI-Pore membrane filters (Structure Probe, no. E1013-MB) and cultured in DMEM/F12 containing N-2 supplement (1 $\times$ ), B-27 supplement (1 $\times$ ), EGF (5 ng/ml), and ampicillin (10  $\mu$ g/ml). Two hours later, the media was switched to culture media containing  $5 \times 10^{10}$  GC/ml Anc80-TRIM71 or Anc80-Ctrl AAV particles. After 48 h of incubation, the culture medium was changed and LY411575 (5  $\mu$ M) was added. Culture medium was exchanged every 2 days.

#### RNA extraction, RT-qPCR, and TaqMan assay

Organoids were harvested using Cell Recovery Solution. Total RNA from organoids/tissue was extracted using the miRNeasy Micro Kit (QIAGEN, no. 217084). mRNA was reverse transcribed into cDNA using the iScript cDNA synthesis kit (Bio-Rad, no. 1708889). Q-PCR was performed on a CFX-Connect Real-Time PCR Detection System (Bio-Rad) using SYBR Green Master Mix reagent (Thermo Fisher Scientific, no. 4385612). Gene-specific qPCR primers are listed in the Reagents and Tools table. *Rpl19* was used as an endogenous reference gene for mRNA quantification. Relative gene expression was calculated using  $2^{-\Delta\Delta C(T)}$  method (Livak & Schmittgen, 2001). To quantify the expression of mature *let-7a-5p*, *let-7d-5p*, *let-7g-5p*, *let-7i-5p* miRNAs, predesigned TaqMan Assays (Applied Biosystems) were used according to the manufacturer's instructions. The snoRNA U6 was used as an endogenous reference gene for TaqMan-based miRNA measurements.

#### RNA sequencing and data analysis

Cochlear epithelial cells from stage P5 wild-type mice were used to establish organoid cultures. Before plating, cells were transduced with control lentivirus (3xHA-T2A-mCherry) or lentivirus expressing human *TRIM71* (3xHA-TRIM71-T2A-mCherry). For each condition, three independent cultures were established. At 10 days of expansion, RNA was extracted, and samples were processed using Illumina's TruSeq stranded Total RNA kit, per manufacturer's recommendations, using the UDI indexes. The samples were sequenced on the NovaSeq 6000, paired end, 2  $\times$  50 base pair reads. Library preparation and sequencing were conducted at the Single Cell & Transcriptomic Core, Johns Hopkins University School of Medicine. Kallisto (v0.46.1) was used to pseudo-align reads to the reference mouse transcriptome and to quantify transcript abundance. The transcriptome index was built using the Ensembl Mus musculus v96 transcriptome. The companion analysis tool Sleuth was used to identify differentially expressed genes (DEGs). We performed a Wald test to produce a list of significant DEGs between *TRIM71* expressing sample and the control. These lists were then represented graphically using Sleuth along with pheatmap and ggplot2 packages in R v1.3.1093. Gene identifier conversion, gene annotation, and enrichment analysis were conducted using Metascape (Zhou et al, 2019).

#### Immunohistochemistry

Acutely isolated cochlear tissue or cultured organoids or explants were fixed in 4% paraformaldehyde for 30 min, permeabilized and

blocked with 0.25% Triton X-100/10% fetal bovine serum for 30 min, and immuno-stained as previously described (Li & Doetzlhofer, 2020; Li et al, 2022). Used antibodies and stains are listed in the [Reagents and Tools table](#).

### Cell proliferation

EdU (Thermo Fisher Scientific, no. C10338) was added to the culture medium at a final concentration of 3  $\mu$ M. EdU incorporation was analyzed using the Click-iTPlus EdU Cell Proliferation Kit (Thermo Fisher Scientific, no. C10637 and C10638) following the manufacturer's recommendations.

### Cell counts

High-power confocal single-plane and z-stack images of fluorescently immuno-labeled organoids and explants were taken with 40 $\times$  objective using LSM 700 confocal microscope (Zeiss Microscopy). To establish the percentage of cells within an organoid that expressed an epitope of interest, at least three images were analyzed, and the average value per animal was reported. At a minimum, two independent experiments were conducted in which at a minimum three organoid cultures per genotype and treatment were established and analyzed.

### Protein lysis co-immunoprecipitation and immunoblotting

HEK 293T cells were transiently transfected with a total of 2.5  $\mu$ g of plasmid DNA. FLAG-Lin28b (Golden et al, 2015) or FLAG-LIN28A (Addgene no. 51371) constructs were co-transfected with 3xHA-TRIM71 expressing constructs using Polyethylenimine, Linear, MW 25000, transfection reagent (Polysciences, no. 23966). After 48 h, cells were lysed in NP-40 lysis buffer (Thermo Scientific, no. J60766.AP) supplemented with protease inhibitor (Roche, no. 11836170001). 1% of cell lysate was saved as input and the remaining lysate was precleared for 1 h with Protein-A Dynabeads (Thermo Scientific, no. 10001D). FLAG-M2 antibody Protein-A Dynabead conjugate was incubated with the precleared lysate overnight. Proteins bound to Protein-A Dynabeads were pulled down using a magnetic separation rack (Cell Signaling, no. 14654). After five washes in NP-40 lysis buffer, beads were resuspended in 4 $\times$  Laemmli protein sample buffer (Bio-Rad, no. 1610747). Protein separation and immunoblots were conducted as previously described (Li & Doetzlhofer, 2020). The resulting chemiluminescence was captured using x-ray films or digitally using LI COR Odyssey imaging system. Cochlear organoids were lysed with RIPA buffer (Sigma-Aldrich, no. R0278) supplemented with protease inhibitor (-Sigma-Aldrich, no. 11697498001), phosphatase inhibitor cocktail 2 (Sigma-Aldrich, no. P5726), and phosphatase inhibitor cocktail 3 (Sigma-Aldrich, no. P0044). Antibodies are listed in the [Reagents and Tools table](#).

### Quantification of organoid forming efficiency, organoid diameter, and GFP<sup>+</sup> cells

Low-power bright-field and fluorescent images of organoid cultures were captured with an Axiovert 200 microscope using 5 $\times$  objectives (Carl Zeiss Microscopy). The organoid formation efficiency and the diameter of organoids were measured as previously described (Li & Doetzlhofer, 2020; Li et al, 2022), and the average value per animal was reported. To establish the percentage of GFP<sup>+</sup> organoids per culture, the total number of organoids and the number of GFP<sup>+</sup> or GFP<sup>+</sup>

mCherry<sup>+</sup> organoids were established by counting manually. For each genotype and treatment, three independent organoid cultures from three different animals were established and analyzed. At a minimum, two independent experiments were conducted and analyzed.

### Statistical analysis

All results were confirmed by at least two independent experiments. The sample size (*n*) represents the number of animals analyzed per group. Animals (biological replicates) were allocated into control or experimental groups based on genotype and/or type of treatment. To avoid bias, blinding and randomization were applied during data analysis. Data were analyzed using GraphPad Prism 8.0. Relevant information for each experiment including sample size, statistical tests, and reported *P* values is found in the legend corresponding to each figure. \**P*  $\leq$  0.05, \*\**P* < 0.01, \*\*\**P* < 0.001, and \*\*\*\**P* < 0.0001. In all cases, *P*-values  $\leq$  0.05 were considered significant, and error bars represent the standard deviation (SD) of biological replicates.

## Data availability

RNA sequencing data have been deposited in the Gene Expression Omnibus data repository under accession number GSE210383 (<http://www.ncbi.nlm.nih.gov/geo/query/acc.cgi?acc=GSE210383>).

**Expanded View** for this article is available [online](#).

### Acknowledgements

We thank the members of the Doetzlhofer Laboratory for the help and advice provided throughout the course of this study. We thank the Single Cell & Transcriptomics Core at Johns Hopkins University School of Medicine for RNA library preparation and sequencing. We thank Dr. Georg Dailey for providing *iLIN28B* transgenic mice. This work has been supported by the National Institute on Deafness and Other Communication Disorders R01DC019359 (AD) and F31DC020882 (CM) and the David M. Rubenstein Fund for Hearing Research (AD). W.K. is funded by the Deutsche Forschungsgemeinschaft under Germany's Excellence Strategy EXC2151-39087304.

### Author contributions

**Xiao-Jun Li:** Conceptualization; data curation; formal analysis; investigation; visualization; methodology; writing – original draft; writing – review and editing. **Charles Morgan:** Formal analysis; validation; investigation; methodology; writing – review and editing. **Prathamesh T Nadar-Ponniiah:** Investigation; methodology. **Waldemar Kolanus:** Resources; writing – review and editing. **Angelika Doetzlhofer:** Conceptualization; data curation; formal analysis; supervision; funding acquisition; writing – original draft; project administration; writing – review and editing.

### Disclosure and competing interests statement

The authors declare that they have no conflict of interest.

## References

- Atkinson PJ, Huarcaya Najarro E, Sayyid ZN, Cheng AG (2015) Sensory hair cell development and regeneration: similarities and differences. *Development* 142: 1561–1571

- Baek S, Tran NTT, Diaz DC, Tsai YY, Acedo JN, Lush ME, Piotrowski T (2022) Single-cell transcriptome analysis reveals three sequential phases of gene expression during zebrafish sensory hair cell regeneration. *Dev Cell* 57: 799–819
- Birmingham NA, Hassan BA, Price SD, Vollrath MA, Ben-Arie N, Eatock RA, Bellen HJ, Lysakowski A, Zoghbi HY (1999) Math1: an essential gene for the generation of inner ear hair cells. *Science* 284: 1837–1841
- Bray NL, Pimentel H, Melsted P, Pachter L (2016) Near-optimal probabilistic RNA-seq quantification. *Nat Biotechnol* 34: 525–527
- Brignull HR, Raible DW, Stone JS (2009) Feathers and fins: non-mammalian models for hair cell regeneration. *Brain Res* 1277: 12–23
- Chai R, Kuo B, Wang T, Liaw EJ, Xia A, Jan TA, Liu Z, Taketo MM, Oghalai JS, Nusse R et al (2012) Wnt signaling induces proliferation of sensory precursors in the postnatal mouse cochlea. *Proc Natl Acad Sci USA* 109: 8167–8172
- Chen J, Lai F, Niswander L (2012) The ubiquitin ligase Mln41 temporally promotes neural progenitor cell maintenance through FGF signaling. *Genes Dev* 26: 803–815
- Chen KS, Lim JWC, Richards LJ, Bunt J (2017) The convergent roles of the nuclear factor I transcription factors in development and cancer. *Cancer Lett* 410: 124–138
- Chen Y, Gu Y, Li Y, Li GL, Chai R, Li W, Li H (2021) Generation of mature and functional hair cells by co-expression of Gfi1, Pou4f3, and Atoh1 in the postnatal mouse cochlea. *Cell Rep* 35: 109016
- Copley MR, Babovic S, Benz C, Knapp DJ, Beer PA, Kent DG, Wohrer S, Treloar DQ, Day C, Rowe K et al (2013) The Lin28b-let-7-Hmga2 axis determines the higher self-renewal potential of fetal haematopoietic stem cells. *Nat Cell Biol* 15: 916–925
- Cuevas E, Rybak-Wolf A, Rohde AM, Nguyen DT, Wulczyn FG (2015) Lin41/Trim71 is essential for mouse development and specifically expressed in postnatal ependymal cells of the brain. *Front Cell Dev Biol* 3: 20
- Duy PQ, Weise SC, Marini C, Li XJ, Liang D, Dahl PJ, Ma S, Spajic A, Dong W, Juusola J et al (2022) Impaired neurogenesis alters brain biomechanics in a neuroprogenitor-based genetic subtype of congenital hydrocephalus. *Nat Neurosci* 25: 458–473
- Evsen L, Li X, Zhang S, Razin S, Doetzlhofer A (2020) Let-7 miRNAs inhibit CHD7 expression and control auditory-sensory progenitor cell behavior in the developing inner ear. *Development* 147: dev183384
- Fedele M, Visone R, De Martino I, Troncone G, Palmieri D, Battista S, Ciarmiello A, Pallante P, Arra C, Melillo RM et al (2006) HMGA2 induces pituitary tumorigenesis by enhancing E2F1 activity. *Cancer Cell* 9: 459–471
- Foster DJ, Chang HM, Haswell JR, Gregory RI, Slack FJ (2020) TRIM71 binds to IMP1 and is capable of positive and negative regulation of target RNAs. *Cell Cycle* 19: 2314–2326
- Golden EJ, Benito-Gonzalez A, Doetzlhofer A (2015) The RNA-binding protein LIN28B regulates developmental timing in the mammalian cochlea. *Proc Natl Acad Sci USA* 112: E3864–E3873
- Gu R, Brown RM II, Hsu CW, Cai T, Crowder AL, Piazza VG, Vadakkan TJ, Dickinson ME, Groves AK (2016) Lineage tracing of Sox2-expressing progenitor cells in the mouse inner ear reveals a broad contribution to non-sensory tissues and insights into the origin of the organ of Corti. *Dev Biol* 414: 72–84
- Jacques BE, Puligilla C, Weichert RM, Ferrer-Vaquer A, Hadjantonakis AK, Kelley MW, Dabdoub A (2012) A dual function for canonical Wnt/ $\beta$ -catenin signaling in the developing mammalian cochlea. *Development* 139: 4395–4404
- Kelly MC, Chang Q, Pan A, Lin X, Chen P (2012) Atoh1 directs the formation of sensory mosaics and induces cell proliferation in the postnatal mammalian cochlea in vivo. *J Neurosci* 32: 6699–6710
- Kiernan AE, Pelling AL, Leung KK, Tang AS, Bell DM, Tease C, Lovell-Badge R, Steel KP, Cheah KS (2005) Sox2 is required for sensory organ development in the mammalian inner ear. *Nature* 434: 1031–1035
- Kolla L, Kelly MC, Mann ZF, Anaya-Rocha A, Ellis K, Lemons A, Palermo AT, So KS, Mays JC, Orvis J et al (2020) Characterization of the development of the mouse cochlear epithelium at the single cell level. *Nat Commun* 11: 2389
- Korrapati S, Roux I, Glowatzki E, Doetzlhofer A (2013) Notch signaling limits supporting cell plasticity in the hair cell-damaged early postnatal murine cochlea. *PLoS ONE* 8: e73276
- Kubota M, Scheibinger M, Jan TA, Heller S (2021) Greater epithelial ridge cells are the principal organoid-forming progenitors of the mouse cochlea. *Cell Rep* 34: 108646
- Landegger LD, Pan B, Askew C, Wassmer SJ, Gluck SD, Galvin A, Taylor R, Forge A, Stankovic KM, Holt JR et al (2017) A synthetic AAV vector enables safe and efficient gene transfer to the mammalian inner ear. *Nat Biotechnol* 35: 280–284
- Lee S, Song JJ, Beyer LA, Swiderski DL, Prieskorn DM, Acar M, Jen HI, Groves AK, Raphael Y (2020) Combinatorial Atoh1 and Gfi1 induction enhances hair cell regeneration in the adult cochlea. *Sci Rep* 10: 21397
- Li XJ, Doetzlhofer A (2020) LIN28B/let-7 control the ability of neonatal murine auditory supporting cells to generate hair cells through mTOR signaling. *Proc Natl Acad Sci USA* 117: 22225–22236
- Li XJ, Morgan C, Goff LA, Doetzlhofer A (2022) Follistatin promotes LIN28B-mediated supporting cell reprogramming and hair cell regeneration in the murine cochlea. *Sci Adv* 8: eabj7651
- Lin YC, Hsieh LC, Kuo MW, Yu J, Kuo HH, Lo WL, Lin RJ, Yu AL, Li WH (2007) Human TRIM71 and its nematode homologue are targets of let-7 microRNA and its zebrafish orthologue is essential for development. *Mol Biol Evol* 24: 2525–2534
- Liu Z, Dearman JA, Cox BC, Walters BJ, Zhang L, Ayrault O, Zindy F, Gan L, Roussel MF, Zuo J (2012) Age-dependent in vivo conversion of mouse cochlear pillar and Deiters' cells to immature hair cells by Atoh1 ectopic expression. *J Neurosci* 32: 6600–6610
- Liu Q, Chen X, Novak MK, Zhang S, Hu W (2021) Repressing Ago2 mRNA translation by Trim71 maintains pluripotency through inhibiting let-7 microRNAs. *Elife* 10: e66288
- Livak KJ, Schmittgen TD (2001) Analysis of relative gene expression data using real-time quantitative PCR and the 2(-Delta Delta C(T)) method. *Methods* 25: 402–408
- Loedige I, Gaidatzis D, Sack R, Meister G, Filipowicz W (2013) The mammalian TRIM-NHL protein TRIM71/LIN-41 is a repressor of mRNA function. *Nucleic Acids Res* 41: 518–532
- Lumpkin EA, Collisson T, Parab P, Omer-Abdalla A, Haeberle H, Chen P, Doetzlhofer A, White P, Groves A, Segil N et al (2003) Math1-driven GFP expression in the developing nervous system of transgenic mice. *Gene Expr Patterns* 3: 389–395
- Maller Schulman BR, Liang X, Stahlhut C, DelConte C, Stefani G, Slack FJ (2008) The let-7 microRNA target gene, Mln41/Trim71 is required for mouse embryonic survival and neural tube closure. *Cell Cycle* 7: 3935–3942
- Mayr C, Hemann MT, Bartel DP (2007) Disrupting the pairing between let-7 and Hmga2 enhances oncogenic transformation. *Science* 315: 1576–1579
- McLean WJ, Yin X, Lu L, Lenz DR, McLean D, Langer R, Karp JM, Edge ASB (2017) Clonal expansion of Lgr5-positive cells from mammalian cochlea and high-purity generation of sensory hair cells. *Cell Rep* 18: 1917–1929
- Medeiros de Araújo JA, Barão S, Mateos-White I, Espinosa A, Costa MR, Gil-Sanz C, Müller U (2021) ZBTB20 is crucial for the specification of a subset

- of callosal projection neurons and astrocytes in the mammalian neocortex. *Development* 148: dev196642
- Mitschka S, Ulas T, Goller T, Schneider K, Egert A, Mertens J, Brustle O, Schorle H, Beyer M, Klee K et al (2015) Co-existence of intact stemness and priming of neural differentiation programs in mES cells lacking Trim71. *Sci Rep* 5: 11126
- Mizutani K, Fujioka M, Hosoya M, Bramhall N, Okano HJ, Okano H, Edge AS (2013) Notch inhibition induces cochlear hair cell regeneration and recovery of hearing after acoustic trauma. *Neuron* 77: 58–69
- Morrison A, Hodgetts C, Gossler A, Hrabe de Angelis M, Lewis J (1999) Expression of Delta1 and Serrate1 (Jagged1) in the mouse inner ear. *Mech Dev* 84: 169–172
- Nguyen DTT, Richter D, Michel G, Mitschka S, Kolanus W, Cuevas E, Wulczyn FG (2017) The ubiquitin ligase LIN41/TRIM71 targets p53 to antagonize cell death and differentiation pathways during stem cell differentiation. *Cell Death Differ* 24: 1063–1078
- Nishino J, Kim I, Chada K, Morrison SJ (2008) Hmga2 promotes neural stem cell self-renewal in young but not old mice by reducing p16Ink4a and p19Arf expression. *Cell* 135: 227–239
- Ohyama T, Basch ML, Mishina Y, Lyons KM, Segil N, Groves AK (2010) BMP signaling is necessary for patterning the sensory and nonsensory regions of the developing mammalian cochlea. *J Neurosci* 30: 15044–15051
- Pimentel H, Bray NL, Puente S, Melsted P, Pachter L (2017) Differential analysis of RNA-seq incorporating quantification uncertainty. *Nat Methods* 14: 687–690
- Reinhart BJ, Slack FJ, Basson M, Pasquinelli AE, Bettinger JC, Rougvie AE, Horvitz HR, Ruvkun G (2000) The 21-nucleotide let-7 RNA regulates developmental timing in *Caenorhabditis elegans*. *Nature* 403: 901–906
- Robinton DA, Chal J, Lummertz da Rocha E, Han A, Yermalovich AV, Oginuma M, Schlaeger TM, Sousa P, Rodriguez A, Urbach A et al (2019) The Lin28/let-7 pathway regulates the mammalian caudal body Axis elongation program. *Dev Cell* 48: 396–405
- Rybak A, Fuchs H, Hadian K, Smirnova L, Wulczyn EA, Michel G, Nitsch R, Krappmann D, Wulczyn FG (2009) The let-7 target gene mouse lin-41 is a stem cell specific E3 ubiquitin ligase for the miRNA pathway protein Ago2. *Nat Cell Biol* 11: 1411–1420
- Shi F, Kempfle JS, Edge AS (2012) Wnt-responsive Lgr5-expressing stem cells are hair cell progenitors in the cochlea. *J Neurosci* 32: 9639–9648
- Shi F, Hu L, Jacques BE, Mulvaney JF, Dabdoub A, Edge AS (2014)  $\beta$ -Catenin is required for hair-cell differentiation in the cochlea. *J Neurosci* 34: 6470–6479
- Sinkkonen ST, Chai R, Jan TA, Hartman BH, Laske RD, Gahlen F, Sinkkonen W, Cheng AG, Oshima K, Heller S (2011) Intrinsic regenerative potential of murine cochlear supporting cells. *Sci Rep* 1: 26
- Sun S, Li S, Luo Z, Ren M, He S, Wang G, Liu Z (2021) Dual expression of Atoh1 and Ikzf2 promotes transformation of adult cochlear supporting cells into outer hair cells. *Elife* 10: e66547
- Takebayashi S, Yamamoto N, Yabe D, Fukuda H, Kojima K, Ito J, Honjo T (2007) Multiple roles of notch signaling in cochlear development. *Dev Biol* 307: 165–178
- Torres Fernández LA, Mitschka S, Ulas T, Weise S, Dahm K, Becker M, Händler K, Beyer M, Windhausen J, Schultze JL et al (2021) The stem cell-specific protein TRIM71 inhibits maturation and activity of the pro-differentiation miRNA let-7 via two independent molecular mechanisms. *RNA* 27: 805–828
- Torres-Fernandez LA, Jux B, Bille M, Port Y, Schneider K, Geyer M, Mayer G, Kolanus W (2019) The mRNA repressor TRIM71 cooperates with nonsense-mediated decay factors to destabilize the mRNA of CDKN1A/p21. *Nucleic Acids Res* 47: 11861–11879
- Torres-Fernandez LA, Emich J, Port Y, Mitschka S, Woste M, Schneider S, Fietz D, Oud MS, Di Persio S, Neuhaus N et al (2021) TRIM71 deficiency causes germ cell loss during mouse embryogenesis and is associated with human male infertility. *Front Cell Dev Biol* 9: 658966
- Vignali R, Marracci S (2020) HMGA genes and proteins in development and evolution. *Int J Mol Sci* 21: 654
- Walters BJ, Coak E, Dearman J, Bailey G, Yamashita T, Kuo B, Zuo J (2017) In vivo interplay between p27(Kip1), GATA3, ATOH1, and POU4F3 converts non-sensory cells to hair cells in adult mice. *Cell Rep* 19: 307–320
- White PM, Doetzlhofer A, Lee YS, Groves AK, Segil N (2006) Mammalian cochlear supporting cells can divide and trans-differentiate into hair cells. *Nature* 441: 984–987
- Winslow MM, Dayton TL, Verhaak RG, Kim-Kiselak C, Snyder EL, Feldser DM, Hubbard DD, DuPage MJ, Whittaker CA, Hoersch S et al (2011) Suppression of lung adenocarcinoma progression by Nkx2-1. *Nature* 473: 101–104
- Worringer KA, Rand TA, Hayashi Y, Sami S, Takahashi K, Tanabe K, Narita M, Srivastava D, Yamanaka S (2014) The let-7/LIN-41 pathway regulates reprogramming to human induced pluripotent stem cells by controlling expression of prodifferentiation genes. *Cell Stem Cell* 14: 40–52
- Yu KR, Shin JH, Kim JJ, Koog MG, Lee JY, Choi SW, Kim HS, Seo Y, Lee S, Shin TH et al (2015) Rapid and efficient direct conversion of human adult somatic cells into neural stem cells by HMG2A/let-7b. *Cell Rep* 10: 441–452
- Zhang S, Qiang R, Dong Y, Zhang Y, Chen Y, Zhou H, Gao X, Chai R (2020) Hair cell regeneration from inner ear progenitors in the mammalian cochlea. *Am J Stem Cells* 9: 25–35
- Zheng JL, Gao WQ (2000) Overexpression of Math1 induces robust production of extra hair cells in postnatal rat inner ears. *Nat Neurosci* 3: 580–586
- Zhou Y, Zhou B, Pache L, Chang M, Khodabakhshi AH, Tanaseichuk O, Benner C, Chanda SK (2019) Metascape provides a biologist-oriented resource for the analysis of systems-level datasets. *Nat Commun* 10: 1523
- Zhu H, Shyh-Chang N, Segre AV, Shinoda G, Shah SP, Einhorn WS, Takeuchi A, Engreitz JM, Hagan JP, Kharas MG et al (2011) The Lin28/let-7 axis regulates glucose metabolism. *Cell* 147: 81–94
- Zou Y, Chiu H, Zinovyeva A, Ambros V, Chuang CF, Chang C (2013) Developmental decline in neuronal regeneration by the progressive change of two intrinsic timers. *Science* 340: 372–376